

Reduced Complexity Model Intercomparison Project Phase 2: Synthesising Earth system knowledge for probabilistic climate projections

Z. Nicholls^{1,2}, M. Meinshausen^{1,2,3}, J. Lewis¹, M. Rojas Corradi^{4,5}, K. Dorheim⁶, T. Gasser⁷, R. Gieseke⁸, A. P. Hope⁹, N. J. Leach¹⁰, L. A. McBride¹¹, Y. Quilcaille⁷, J. Rogelj^{12,7}, R. J. Salawitch^{11,9,13}, B. H. Samset¹⁴, M. Sandstad¹⁴, A. Shiklomanov¹⁵, R. B. Skeie¹⁴, C. J. Smith^{16,7}, S. J. Smith¹⁷, X. Su¹⁸, J. Tsutsui¹⁹, B. Vega-Westhoff²⁰ and D. L. Woodard⁵

¹Australian-German Climate & Energy College, The University of Melbourne, Parkville, Victoria, Australia

²School of Earth Sciences, The University of Melbourne, Parkville, Victoria, Australia

³Potsdam Institute for Climate Impact Research (PIK), Member of the Leibniz Association, Potsdam, Germany

⁴Department of Geophysics, University of Chile, Santiago, Chile

⁵Center for Climate and Resilience Research, CR2, Santiago, Chile

⁶Pacific Northwest National Laboratory

⁷International Institute for Applied Systems Analysis, Laxenburg, Austria

⁸Independent researcher, Potsdam, Germany

⁹Department of Atmospheric and Oceanic Science, University of Maryland-College Park, College Park, 20740, USA

¹⁰Atmospheric, Oceanic, and Planetary Physics, Department of Physics, University of Oxford, United Kingdom

¹¹Department of Chemistry and Biochemistry, University of Maryland-College Park, College Park, 20740, USA

¹²Grantham Institute, Imperial College London, London, UK

¹³Earth System Science Interdisciplinary Center, University of Maryland-College Park, College Park, 20740, USA

¹⁴CICERO Center for International Climate Research, Oslo, Norway

¹⁵NASA Goddard Space Flight Center, Greenbelt, MD, USA 20771

¹⁶Priestley International Centre for Climate, University of Leeds, United Kingdom

¹⁷Joint Global Change Research Institute, Pacific Northwest National Laboratory, College Park, MD, USA

¹⁸Research Institute for Global Change / Research Center for Environmental Modeling and Application / Earth System Model Development and Application Group, Japan Agency for Marine-Earth Science and Technology (JAMSTEC), Yokohama, Japan

¹⁹Environmental Science Research Laboratory, Central Research Institute of Electric Power Industry, Abiko, Japan

²⁰Department of Atmospheric Sciences, University of Illinois at Urbana-Champaign, Urbana, IL, USA

Key Points:

- Probabilistic global-mean temperature projections often use reduced complexity climate models (RCMs) because of their low computational cost
- We evaluate how well RCMs' probabilistic setups can synthesise knowledge from multiple research domains for policy relevant projections
- No RCM is able to capture all forcing, warming, heat uptake and carbon cycle metrics we evaluate, however some come close across a range

Corresponding author: Zebedee Nicholls, zebedee.nicholls@climate-energy-college.org

Abstract

Over the last decades, climate science has evolved rapidly across multiple expert domains. Our best tools to capture state-of-the-art knowledge in an internally self-consistent modelling framework are the increasingly complex fully coupled Earth System Models (ESMs). However, computational limitations and the structural rigidity of ESMs mean that the full range of uncertainties across multiple domains are difficult to capture with ESMs alone. The tools of choice are instead more computationally efficient reduced complexity models (RCMs), which are structurally flexible and can span the response dynamics across a range of domain-specific models and ESM experiments. Here we present Phase 2 of the Reduced Complexity Model Intercomparison Project (RCMIP Phase 2), the first comprehensive intercomparison of RCMs that are probabilistically calibrated with key benchmark ranges from specialised research communities. Unsurprisingly, but crucially, we find that models which have been constrained to reflect the key benchmarks better reflect the key benchmarks. Under the low-emissions SSP1-1.9 scenario, across the RCMs, median peak warming projections range from 1.3 to 1.7°C (relative to 1850-1900, using an observationally-based historical warming estimate of 0.8°C between 1850-1900 and 1995-2014). Further developing methodologies to constrain these projection uncertainties seems paramount given the international community's goal to contain warming to below 1.5°C above pre-industrial in the long-term. Our findings suggest that users of RCMs should carefully evaluate their RCM, specifically its skill against key benchmarks and consider the need to include projections benchmarks either from ESM results or other assessments to reduce divergence in future projections.

Plain Language Summary

Our best tools to capture state-of-the-art knowledge are complex, fully coupled Earth System Models (ESMs). However, ESMs are expensive to run and no single ESM can easily produce responses which represent the full range of uncertainties. Instead, for some applications, computationally efficient reduced complexity climate models (RCMs) are used in a probabilistic setup. An example of these applications is estimating the likelihood that an emissions scenario will stay below a certain global-mean temperature change. Here we present a study (referred to as the Reduced Complexity Model Intercomparison Project (RCMIP) Phase 2) which investigates the extent to which different RCMs can be probabilistically calibrated to reproduce knowledge from specialised research communities. We find that the agreement between each RCM and the benchmarks varies, although the best performing models show good agreement across the majority of benchmarks. Under a very-low emissions scenario median peak warming projections range from 1.3 to 1.7°C (relative to 1850-1900, assuming historical warming of 0.8°C between 1850-1900 and 1995-2014). Investigating new ways to reduce these projection uncertainties seems paramount given the international community's goal to limit warming to below 1.5°C above pre-industrial in the long-term.

1 Introduction

Coupled Earth System Models (ESMs) have evolved for decades as primary climate research tools (Kawamiya et al., 2020). They represent the state of the art of complex Earth system modelling. Nonetheless, they are not the tool of choice to assess the full breadth of scenario and Earth system response uncertainty that has been identified in the scientific literature. It is infeasible to assess the climate implications of hundreds to thousands of emissions scenarios with the world's most comprehensive ESMs, such as those participating in the Sixth Phase of the Couple Model Intercomparison Project (CMIP6) (Eyring et al., 2016), because of ESMs' computational cost, the complexity in setting up input data and the sheer volume of output data generated. Yet, large scenario assess-

95 ments are vital for understanding the consequences of various policy choices and their
96 residual climate hazards.

97 Similarly, while some ESMs perform large, perturbed physics experiments (e.g., Mur-
98 phy et al., 2014) that aim to explore a range of potential Earth system long-term annual-
99 average responses, the ability to capture full uncertainty ranges is limited. The ability
100 to capture full uncertainty ranges is limited because these ESMs are relatively rigid in
101 their structure - lacking the ability to completely explore uncertainties in vital compo-
102 nents like the carbon cycle or effective radiative forcings.

103 An answer to both of these challenges, i.e. (a) limited computational resources and
104 (b) structural scope and flexibility to represent long-term uncertainties in key metrics
105 like global-mean surface air temperatures, are Reduced Complexity Models (RCMs), of-
106 ten also referred to as simple climate models (SCMs). RCMs can play the vital role of
107 extending the knowledge and uncertainties from multiple domains, particularly a mul-
108 titude of ESM experiments, to probabilistic long-term climate projections of key vari-
109 ables over a wide range of scenarios. Earth System Models of Intermediate Complexity
110 (EMICs) may initially appear to be another option. However, due to the process-based
111 representations used by EMICs, their computational complexity and data requirements
112 are still orders of magnitude greater than RCMs. As a result, even EMICs are not a fea-
113 sible choice for the large-scale, probabilistic assessment discussed here.

114 Typically, RCMs achieve computational efficiency and structural flexibility by lim-
115 iting their spatial and temporal domains to global-mean, annual-mean quantities i.e the
116 domains of relevance to long-term, global climate change. In general, RCMs don't in-
117 clude representations of interannual variability, although the EMGC model (Table 1) is
118 a clear exception to this rule. Rather than aiming to represent the physics of the climate
119 system at the process level and high-resolution, RCMs use parameterisations of the sys-
120 tem which capture its large-scale behaviour at a greatly reduced computational cost. This
121 allows them to perform 350-year long simulations in a fraction of a second on a single
122 CPU, multiple orders of magnitude faster than our most comprehensive ESMs which would
123 take weeks to months on the world's most advanced supercomputers.

124 A key example of large-scale emissions scenario assessment, and the one we focus
125 on in this paper, is the climate assessment of socioeconomic scenarios by the Intergov-
126 ernmental Panel on Climate Change (IPCC) Working Group 3 (WG3). Hundreds of emis-
127 sion scenarios were assessed in the IPCC's Fifth Assessment Report (AR5, see Clarke
128 et al. (2014)) as well as its more recent Special Report on Global Warming of 1.5°C (SR1.5,
129 see Rogelj et al. (2018); Huppmann et al. (2018)). (Scenario data is available at [https://
130 secure.iiasa.ac.at/web-apps/ene/AR5DB](https://secure.iiasa.ac.at/web-apps/ene/AR5DB) and [https://data.ene.iiasa.ac.at/iamc
131 -1.5c-explorer/](https://data.ene.iiasa.ac.at/iamc-1.5c-explorer/) for AR5 and SR1.5 respectively, both databases are hosted by the IIASA
132 Energy Program). For the IPCC's forthcoming Sixth Assessment (AR6), it is anticipated
133 that the number of scenarios will be in the several hundreds to a thousand (an initial
134 snapshot of scenarios based on the SSPs is available at [https://tntcat.iiasa.ac.at/
135 SspDb](https://tntcat.iiasa.ac.at/SspDb)).

136 Running WG3-type scenarios requires at least some representation of greenhouse
137 gas cycles, atmospheric chemistry and dynamic vegetation modules. While some of the
138 world's most comprehensive ESMs have the required components, they could not be used
139 to sample scenario and parametric uncertainty for reasons of computational cost. The
140 most comprehensive RCMs include parameterised representations of the required compo-
141 nents (including feedbacks of climate on permafrost and wetland methane emissions),
142 enabling the exploration of interacting uncertainties from multiple parts of the climate
143 system in an internally consistent setup.

144 While RCMs do not include the detail of ESMs across the emissions-climate change
145 cause-effect chain, they do tend to include uncertainty representations for more steps in

146 the chain (i.e. RCMs tradeoff depth for breadth compared to ESMs). For example, many
147 RCMs include the relationship between methane emissions and concentrations (includ-
148 ing temperature and other feedbacks) whereas few ESMs do in their long-term exper-
149 iments. On the other hand, few RCMs directly use land-cover information within their
150 carbon cycles, and none consider it in the detailed way which ESMs do. In addition, there
151 are clearly applications where RCMs are not a feasible tool. For example, near-term at-
152 tribution studies, such as the World Weather Attribution project (Uhe et al., 2016). For
153 this latter application, large-ensemble ESM runs are vital - as only they can reflect nat-
154 ural variability and weather patterns. Overall, there is no question that ESMs are by far
155 the most important research tool to project future climate change. RCMs complement
156 the ESM efforts. Within this paper, we focus on a very specific niche of this complement-
157 ing role, i.e. the degree to which RCMs can synthesise multiple lines of evidence across
158 the emissions-climate change cause-effect chain.

159 Typically, RCMs attempt to perform this synthesis using probabilistic parameter
160 ensembles (see also Section 3), which are distinct from the emulator mode in which RCMs
161 can also be run (see Z. R. J. Nicholls et al. (2020) for a discussion of emulation with RCMs).
162 These probabilistic parameter ensembles are derived based on knowledge of specific Earth
163 system quantities drawn from multiple, often independent, research communities, e.g.
164 historical global mean temperature increase, effective radiative forcing due to different
165 anthropogenic emissions, ocean heat uptake, or cumulative land and ocean carbon up-
166 take. The resulting distributions can then be used in a variety of applications, e.g. to
167 assess the likelihood that different warming levels are reached under a specific emissions
168 scenario (e.g. 50% and 66%) based on the combined available evidence. As a result of
169 their probabilistic nature, the ensembles resulting from RCMs are conceptually differ-
170 ent from an ensemble of multiple model outputs that has not been constructed with any
171 relative probabilities in mind (such as those from CMIP6) taken without constraining
172 or any other sort of post-processing.

173 Within the IPCC, RCMs' synthesising niche facilitates the transfer of knowledge
174 from Working Group I (WG1), which assesses the physical science of the climate sys-
175 tem, to WG3, which assesses the socioeconomics of climate change mitigation. The goal
176 of this knowledge transfer is consistency between WG3's scenario classification and the
177 physical science assessment of WG1 - a key precondition to have confidence that WG3's
178 conclusions about the socioeconomic transformation required to mitigate anthropogenic
179 climate change to specific levels are based on our latest scientific understanding. Here,
180 we describe RCMs as 'integrators of knowledge' because they integrate (a relevant sub-
181 section of) the assessment from WG1, providing WG3 with a tool that can be used for
182 assessing the climate implications, particularly global-mean temperature changes, of a
183 wide range of emissions scenarios.

184 Due to their role in the IPCC assessment (and for analysing mitigation options in
185 line with temperature targets more generally), understanding the degree to which RCMs
186 can reflect a range of independent radiative forcing, warming, heat uptake and concen-
187 tration assessments simultaneously is of vital importance. Given that these assessments
188 are independent, a single, internally consistent, model may not be able to capture them
189 all. If RCMs are inherently biased in some way or they are unable to simultaneously cap-
190 ture the independent assessments, this will affect the WG3 climate assessment and in-
191 terpretation of the RCMs' outputs should be adjusted accordingly.

192 This study's scope, in terms of number of climate dimensions considered and num-
193 ber of climate models evaluated, is unique. While there have been studies with single
194 models which choose parameter sets that match various assessments of ECS and TCR
195 (e.g. Meinshausen et al., 2009; Rogelj et al., 2012) and Smith, Forster, et al. (2018) com-
196 pared two models' probabilistic outputs, no previous study into RCM probabilistic dis-
197 tributions is of the same breadth.

198 Here, in the second phase of RCMIP, we evaluate the degree to which multiple RCMs
199 are able to synthesise Earth system knowledge within a probabilistic distribution. We
200 then examine the implications of differences in these probabilistic distributions for cli-
201 mate projections. We extend previous probabilistic evaluation work and build on the progress
202 made in the first phase of RCMIP (Z. R. J. Nicholls et al., 2020) and other RCM inter-
203 comparison studies (van Vuuren et al., 2011; Harmsen et al., 2015; Schwarber et al., 2019).
204 We widen the first phase's scope both in terms of number of climate dimensions consid-
205 ered and the number of models evaluated. To our knowledge, this is the most compre-
206 hensive evaluation performed to date of the ability of RCMs to capture a broad range
207 of climate metrics and key indicators, such as those assessed in by IPCC WG1.

208 **2 Participating models**

209 Nine models have participated in RCMIP Phase 2 (Table 1 and Supplementary Text
210 S1). Models were invited to participate via an open invitation made available at `rcmip`
211 `.org` and circulated via relevant researcher networks. All interested modelling teams were
212 included. These models and their components range from simpler, regression-based ap-
213 proaches to more complex representations with detailed processes and regions. The mod-
214 els have been constrained in a number of different ways, using statistical techniques rang-
215 ing in complexity from Monte Carlo Markov Chains to using pass/fail criteria to deter-
216 mine valid parameter values. As a result, the models and techniques cover (to the best
217 of our knowledge) the full range of techniques seen in the literature and their results al-
218 low us to evaluate the implications of different choices.

219 **3 Methods**

220 In this study, the RCMs are run in a probabilistic setup, also referred to as a prob-
221 abilistic distribution. As discussed in the introduction, a probabilistic setup means that
222 each RCM is run with an ensemble of parameter configurations. Specifically, for a given
223 experiment, each RCM is run multiple times, each time in a different configuration i.e.
224 with different parameter values. All of these different runs are then combined to form
225 a probabilistic set of outputs. With these probabilistic sets, we can then calculate ranges
226 of each output variable of interest (e.g. global-mean surface temperatures).

227 Modelling groups use a range of techniques to derive their parameter ensembles i.e.
228 to constrain their models (Table 1). In each probabilistic run, the parameter ensemble
229 is fixed i.e. the same set of parameter configurations will be used in each experiment.
230 This choice ensures that the model outputs are deterministic, rather than including a
231 random element due to e.g. sampling parameter values from a range or probability dis-
232 tribution for each run. Typically, modelling groups will also use different data to derive
233 their parameter ensemble. This can lead to differences in model projections which are
234 simply based on choices made by the modelling groups and are not related to model struc-
235 ture or constraining technique at all. In this study, two models (MAGICC7 and MCE-
236 v1-2) have used a common set of target assessed ranges, i.e. benchmarks, to derive their
237 probabilistic distributions. For these models, we are able to rule out the choice of data
238 as the cause of difference between these models. Accordingly, we can more clearly iden-
239 tify the importance of model structure and constraining technique for future projections.

240 In this study, our target assessment is a 'proxy assessment', which uses assessed
241 climate system characteristics in line with IPCC AR5 as its starting point and updates
242 key values using more recent literature (Table 2). We explicitly use the name 'proxy as-
243 sessment' throughout to make clear that we are not constraining to any ranges coming
244 from the formal IPCC assessment, rather an approximation thereof. Notably, in this study,
245 the proxy assessment does not include any future projections. While we examine future
246 projections coming from the models, we do not explicitly compare them against future
247 projections coming from another line of evidence because there is no obvious choice for

Table 1. Overview of the models and constraining approaches used in this paper. Detailed descriptions of each model are available in Supplementary Text S1.

| Model | Constraining technique | Key references |
|------------------|--|---|
| CICERO-SCM | 591 members sub-sampled from a posterior of 30 040 members to form a set that match the proxy assessment ocean heat content distribution while excluding parameter sets with unrealistic aerosol ERF or unrealistic surface air temperature change from 1850-1900 to 1985-2014 | Schlesinger et al. (1992); Joos et al. (1996); Etminan et al. (2016); Skeie et al. (2017, 2018); Z. R. J. Nicholls et al. (2020); Skeie et al. (2021) |
| EMGC | 160 000 sample members, retaining the 1 000 that minimize reduced-chi-squared between modeled and observed GMST and OHC from 1850-1999 | Canty et al. (2013); Hope et al. (2017, 2020); McBride et al. (2020) |
| FaIRv1.6.1 | 3 000 sample members retaining the 501 that minimise RMSE between modelled and observed 1850-2014 GMST | Millar et al. (2017); Smith, Forster, et al. (2018) |
| FaIRv2.0.0-alpha | 1 million member raw ensemble, constrained with likelihood of 2010-2019 level and rate of attributable warming, calculated using the Global Warming Index methodology (Haustein et al., 2017). 5000 members randomly drawn from the constrained ensemble for use here. | Millar et al. (2017); Haustein et al. (2017); Smith, Forster, et al. (2018); Leach et al. (2020) |
| Hectorv2.5.0 | 10 000 sampled ensemble from Markov chain Monte Carlo chains constrained with global surface temperature and ocean heat content | Vega-Westhoff et al. (2019) |
| MAGICCv7.5.1 | 7 million member Monte Carlo Markov Chain, 600 member sub-sample selected to match proxy assessed ranges | Meinshausen et al. (2009, 2011, 2020) |
| MCE v1.2 | 600 members sampled with a Metropolis-Hastings algorithm through Bayesian updating to reflect an ensemble of complex climate models constrained with the proxy assessed ranges | Tsutsui (2017, 2020) (see also Joos et al. (1996); Hooss et al. (2001)) |
| OSCARv3.1 | 10 000 Monte Carlo members, weighted using their agreement with a set of assessed ranges (Supplementary Text S1) | Gasser et al. (2017, 2018, 2020) |
| SCM4OPT v2.1 | For each emission scenario, 2 000 sample members are used to reflect uncertainties resulting from carbon cycle, aerosol forcings and temperature change, while constrained by the historical mean surface temperature of HadCRUT.4.6.0.0 (Morice et al., 2012). | Su et al. (2017, 2018, 2020) |

Table 2. The proxy assessed ranges used in this study. The assessed ranges are labelled as ‘vll’ (very-likely lower i.e. 5th percentile), ‘ll’ (likely lower, 17th percentile), ‘c’ (central, 50th percentile), ‘lu’ (likely upper, 83th percentile) and ‘vlu’ (very-likely upper, 95th percentile). Sources are described in Section 3.

| Metric | Assessed range Unit | vll | ll | c | lu | vlu |
|---|------------------------|------|-------|-------|-------|------|
| 2000-2019 GMST rel. to 1961-1990 | K | 0.46 | | 0.54 | | 0.61 |
| Equilibrium Climate Sensitivity | K | 2.30 | 2.60 | 3.10 | 3.90 | 4.70 |
| Transient Climate Response | K | 0.98 | 1.26 | 1.64 | 2.02 | 2.29 |
| Transient Climate Response to Emissions | K / TtC | 1.03 | 1.40 | 1.77 | 2.14 | 2.51 |
| 2014 CO ₂ Effective Radiative Forcing | W / m ² | | 1.69 | 1.80 | 1.91 | |
| 2014 Aerosol Effective Radiative Forcing | W / m ² | | -1.37 | -1.01 | -0.63 | |
| 2018 Ocean Heat Content rel. to 1971 | ZJ | | 303 | 320 | 337 | |
| 2011 CH ₄ Effective Radiative Forcing | W / m ² | | 0.47 | 0.60 | 0.73 | |
| 2011 N ₂ O Effective Radiative Forcing | W / m ² | | 0.14 | 0.17 | 0.20 | |
| 2011 F-Gases Effective Radiative Forcing | W / m ² | | 0.03 | 0.03 | 0.03 | |

248 such a line of evidence - apart from the ‘assessed ranges’ of SSP scenarios that will be
 249 communicated in the forthcoming IPCC report (but are not available for this study). As
 250 discussed in more detail in Section 4.3, the inclusion of future projections in the proxy
 251 assessment would narrow the range of model projections but any such narrowing should
 252 be carefully considered because - depending on the types of constraints - it may lead to
 253 underestimates of uncertainty.

254 In order to keep the study’s scope manageable, our proxy assessment focuses on
 255 climate response parameters, with the carbon cycle examined only via the TCRE. We
 256 aim to perform a detailed analysis on carbon cycle response in the next phase of RCMIP.

257 We use surface air ocean blended temperatures from the HadCRUT.4.6.0.0 dataset
 258 (Morice et al., 2012). HadCRUT4.6.0.0 is a widely used observational data product and
 259 is representative of other observations of changes in surface air and ocean temperatures
 260 (Simmons et al., 2017). Our key metric for evaluating RCM temperature projections is
 261 the warming between the 1961-1990 and 2000-2019 periods (using the SSP2-4.5 scenario
 262 to extend the CMIP6 historical experiment to 2019). We choose a relatively recent pe-
 263 riod to match the increase in global observations since the 1960s.

264 For ocean heat content, we use the recent work of von Schuckmann et al. (2020).
 265 We focus on the change in ocean heat content between 1971 and 2018, when the largest
 266 set of observations are available.

267 We use the recent assessment of Sherwood et al. (2020) for equilibrium climate sen-
 268 sitivity (ECS). ECS is defined as the equilibrium warming which occurs under a dou-
 269 bling of atmospheric CO₂ concentrations relative to pre-industrial concentrations. The
 270 ECS assessment is combined with the constrained transient climate response (TCR) as-
 271 sessment of Tokarska et al. (2020). TCR is defined as the surface air temperature change
 272 which occurs at the time at which atmospheric CO₂ concentrations double in an exper-
 273 iment in which atmospheric CO₂ concentrations rise at one percent per year (a 1pctCO₂
 274 experiment). Carbon cycle behaviour is considered only via the transient climate response
 275 to emissions (TCRE). TCRE is defined as the ratio of surface air temperature change
 276 to cumulative CO₂ emissions at the time when atmospheric CO₂ concentrations double
 277 in a 1pctCO₂ experiment. We use the TCRE assessment from Arora et al. (2020), which
 278 is based on the latest generation of Earth System Models which have participated in CMIP6

(Eyring et al., 2016). There is a potential inconsistency between our ECS, TCR and TCRE ranges, which arises because the ECS assessment comes from a study which uses multiple lines of evidence, the TCR assessment is based on a constrained set of CMIP6 models and the TCRE assessment is based on unconstrained CMIP6 Earth System Models. We discuss the importance of this inconsistency and its consequences in Section 4.

The other key metrics are related to effective radiative forcing (ERF, Forster et al., 2016). These values generally follow the AR5 assessment, except for aerosol, CO₂ and methane ERF. For aerosol and CO₂ ERF, we use the more recent work of Smith et al. (2020). For methane ERF, we increase the AR5 assessment following Etminan et al. (2016) although we note that this increase may be offset by an updated understanding of the impact of rapid adjustments (Smith, Kramer, et al., 2018).

At this point, we stress that our proxy assessed ranges are only one of a range of possible choices. Assessing all the available literature is a demanding task that is well undertaken by the IPCC. We do not attempt to reproduce this task here. Instead, the key is that our proxy assessed ranges are a) reasonable and b) were available at the time of the study's inception.

Following this intercomparison consortium's choice of proxy assessed ranges, modelling groups then had the opportunity to develop parameter ensembles which best reflected these assessed ranges. As previously discussed, this allowed some modelling teams (although crucially not all) to use the same 'constraining benchmarks' (with a number of different techniques being employed to consider the constraining benchmarks, see Table 1). We use these consistently constrained models to gain unique insights into the impact of differences in model structure and constraining techniques when RCMs are used as integrators of knowledge, free from a typical source of disagreement between the models, namely that they were constrained to reproduce different understandings of the climate. The inclusion of results from models which were not constrained using the same benchmarks allows us to quantify the importance of constraining when using reduced complexity climate models as integrators of knowledge.

The modelling groups submitted a range of concentration-driven, emission-driven and idealized scenarios for their chosen parameter subsets (see scenario specifics below). Subsequently, several metrics were calculated, such as TCR from the idealised CO₂-only 1pctCO2 experiment (in which atmospheric CO₂ concentrations rise at 1% per year from pre-industrial levels). Calculating derived metrics on each individual ensemble member ensures that all metrics are calculated from internally self-consistent model runs, which is of particular importance when the metric is based on more than one output variable from the model (e.g. TCRE, which relies on both surface air temperature change and inverse emissions of CO₂). If we instead calculated results based on percentiles of different variables, we would not be using an internally self-consistent set. Where modelling groups felt it was more appropriate (e.g. OSCARv3.1), they performed their own weighting of ensemble members before submitting.

The one metric which is not easily calculated from model results is ECS because it is defined at equilibrium. Accordingly, modelling groups reported their own diagnosed ECS for each ensemble member, rather than performing experiments which would allow it to be calculated after submission had taken place.

When evaluating model performance, we are interested not only in how well a model can reproduce the best estimate, but also the range, of a given quantity. A key part of any climate assessment is the uncertainty and it is critical that RCMs reflect the assessed likely and very likely ranges if they are to be used as integrators of knowledge. We assess the relative difference between the model and the assessed ranges at the very likely lower (5th percentile, also referred to as 'vll'), likely lower (17th percentile, 'll'), central (50th percentile, 'c'), likely upper (83th percentile, 'lu') and very likely upper (95th per-

centile, 'vlu'). Assessing deviations using relative differences allows us to quickly evaluate how models perform over a range of metrics on the same scale.

The set of scenarios that each modelling group was asked to run follow the experimental protocols of CMIP6's ScenarioMIP (O'Neill et al., 2016). The SSPX-Y.Y experiments (e.g. SSP1-1.9, SSP2-4.5, SSP5-8.5) are defined in terms of concentrations of well-mixed greenhouse gases i.e. CO₂, CH₄, N₂O, hydrofluorocarbons (HFCs), perfluorocarbons (PFCs) and hydrochlorofluorocarbons (HCFCs), emissions of 'aerosol precursor species emissions' i.e. sulfur, nitrates, black carbon, organic carbon and ammonia and natural effective radiative forcing variations. As described in Z. R. J. Nicholls et al. (2020), where required, models may use prescribed effective radiative forcing if they do not include the required gas cycles or radiative forcing parameterisations.

The esm-SSPX-Y.Y experiments are identical to the SSPX-Y.Y experiments, except CO₂ emissions are prescribed instead of CO₂ concentrations, following the CMIP6 C4MIP protocol (Jones et al., 2016). Finally, we also perform esm-SSPX-Y.Y-allGHG experiments. These are identical to the esm-SSPX-Y.Y experiments, except they are defined in terms of emissions of all well-mixed greenhouse gases, not only CO₂, rather than concentrations. There is no equivalent of these esm-SSPX-Y.Y-allGHG experiments in the CMIP6 protocol, however it is these experiments which are of most interest to WG3, given that WG3 focuses on scenarios defined in terms of emissions alone. We use the data sources described in Z. R. J. Nicholls et al. (2020) to specify the inputs for each of these scenarios. The input dataset compilations, comprising emission, scenario and forcing data, as well as the protocols are archived with Zenodo (Z. Nicholls & Lewis, 2021) - and can contribute to scientific studies beyond this intercomparison as they largely reflect the CMIP6 experimental designs.

The protocol designed for this study requires that each RCM modelling group runs every probabilistic ensemble member once for each scenario and then submits their output for further analysis. With nine modelling groups participating, this intercomparison project compiled a database of results containing thousands of runs for each RCM, from which we can calculate different warming, effective radiative forcing or ocean heat uptake percentiles for a wide range of scenarios.

4 Results and discussion

4.1 Fit to assessed ranges

The ability of RCMs to match the assessed ranges varies (Table 3, Figure 1, Supplementary Table S1 and Supplementary Figures S1 - S9). In general, the RCMs capture the central assessed values better than the likely and very likely ranges. Historical warming, TCR and the TCRE are notable exceptions to this. For the TCR, the upper likely and very likely upper assessed values are captured by the RCMs about as well as the central value. For TCRE and historical warming, the very likely lower and likely lower assessed values are better captured by the RCMs than the central values.

Considering the variation between metrics, we see that the proxy assessment of the ocean heat content and effective radiative forcing metrics is better captured by the RCMs than the other metrics. For the ocean heat content and effective radiative forcing metrics, the median multi-model difference is less than or equal to 10% for the central proxy assessed range. However, there is less close agreement with the very likely and likely proxy assessed ranges for the effective radiative forcing metrics, with median multi-model differences being up to 19% (aerosol effective radiative forcing).

For the other metrics (historical warming, ECS, TCR and TCRE), the median multi-model difference is greater than 20% for at least one of the assessed ranges. However, there is significant variation across the likelihood levels. For example, the multi-model

Table 3. Comparison of each model's probabilistic distribution with the proxy assessment. In each square, we show the relative difference between the model result and the proxy assessed value (Δ_m , calculated as $\Delta_m = \frac{m-a}{|a|}$ where m is the value from the model's probabilistic distribution and a is the proxy assessment value). Bold cells indicate that this model is within 20% of the proxy assessment at all likelihood levels for this metric. If a row is completely empty for a model, this indicates that the model did not submit results which allowed that metric to be calculated. Empty cells within a row which is otherwise not completely empty for a model indicates that no proxy assessment at this likelihood level was available (e.g. we have proxy assessments for likely lower 2014CO₂ effective radiative forcing, but not for very likely lower 2014CO₂ effective radiative forcing). Only the magnitude of Δ_m from each model was used to calculate the multi-model median (to ensure that positive and negative values of Δ_m from different models would not cancel out). The assessed ranges are labelled as 'vll' (very-likely lower i.e. 5th percentile), 'll' (likely lower, 17th percentile), 'c' (central, 50th percentile), 'lu' (likely upper, 83th percentile) and 'vlu' (very-likely upper, 95th percentile). (Note, continues on next page.)

| Climate model Assessed range | Multi-model median of magnitude of relative differences | | | | | | | | | | | | | | |
|---|---|------------|------------|-------------|------------|------|------------|------------|------------|------|------------|------------|-------------|-------------|-------------|
| | vll | ll | c | lu | vlu | vll | ll | c | lu | vlu | | | | | |
| 2000-2019 GMST rel. to 1961-1990 | 7% | | 11% | | 25% | | | | | | | | | | |
| Equilibrium Climate Sensitivity | 16% | 15% | 12% | 14% | 20% | | | | | | | | | | |
| Transient Climate Response | 38% | 18% | 7% | 4% | 7% | | | | | | | | | | |
| Transient Climate Response to Emissions | 9% | 11% | 20% | 19% | 20% | | | | | | | | | | |
| 2014 CO ₂ Effective Radiative Forcing | | 5% | 5% | 1% | | | | | | | | | | | |
| 2014 Aerosol Effective Radiative Forcing | | 14% | 10% | 19% | | | | | | | | | | | |
| 2018 Ocean Heat Content rel. to 1971 | | 1% | 1% | 16% | | | | | | | | | | | |
| 2011 CH ₄ Effective Radiative Forcing | | 4% | 6% | 18% | | | | | | | | | | | |
| 2011 N ₂ O Effective Radiative Forcing | | 11% | 2% | 10% | | | | | | | | | | | |
| 2011 F-Gases Effective Radiative Forcing | | 2% | 3% | 4% | | | | | | | | | | | |
| Climate model Assessed range | CICERO-SCM | | | | | EMGC | | | | | FaIR1.6 | | | | |
| | vll | ll | c | lu | vlu | vll | ll | c | lu | vlu | vll | ll | c | lu | vlu |
| 2000-2019 GMST rel. to 1961-1990 | 6% | | 12% | | 17% | -30% | | -11% | | 35% | 14% | | 23% | | 37% |
| Equilibrium Climate Sensitivity | 9% | 4% | -2% | -12% | -22% | -43% | -42% | -38% | -28% | -12% | -16% | -11% | -3% | 11% | 32% |
| Transient Climate Response | 33% | 14% | 1% | -6% | -12% | | | | | | 43% | 23% | 10% | 5% | 8% |
| Transient Climate Response to Emissions | | 15% | 8% | 2% | | | 12% | 6% | -0% | | 17% | -3% | -10% | -11% | -12% |
| 2014 CO ₂ Effective Radiative Forcing | | 28% | 37% | 64% | | | 16% | 16% | 16% | | | 2% | 0% | -4% | |
| 2014 Aerosol Effective Radiative Forcing | | 0% | -0% | -0% | | | -9% | 2% | 26% | | | -0% | 12% | 24% | |
| 2018 Ocean Heat Content rel. to 1971 | | 12% | -12% | -27% | | | 23% | -3% | -20% | | | 3% | -8% | -15% | |
| 2011 CH ₄ Effective Radiative Forcing | | 13% | -6% | -20% | | | 25% | 4% | -12% | | | 8% | -2% | -9% | |
| 2011 N ₂ O Effective Radiative Forcing | | | | | | | | | | | | -1% | -3% | -4% | |
| 2011 F-Gases Effective Radiative Forcing | | | | | | | | | | | | | | | |

Table 3. (Continued.)

| Climate model Assessed range | FaIRv2.0.0-alpha | | | | Hector | | | | MAGICCv7.5.1 | | | | | |
|---|------------------|------|------|------|-----------|------|------|------|--------------|------|------|------|------|------|
| | vll | ll | c | lu | vlu | vll | ll | c | lu | vll | ll | c | lu | vlu |
| 2000-2019 GMST rel. to 1961-1990 | 11% | | 22% | 38% | 7% | 16% | 25% | 1% | 1% | 1% | 1% | 1% | 1% | 2% |
| Equilibrium Climate Sensitivity | -22% | -15% | -2% | 15% | -20% | -8% | 16% | -13% | -14% | -15% | -16% | -16% | -16% | -17% |
| Transient Climate Response | 26% | 12% | 4% | 3% | 45% | 11% | 3% | 32% | 7% | 16% | 7% | 2% | 2% | 0% |
| Transient Climate Response to Emissions | -1% | -16% | -20% | -19% | -20% | | | 9% | -1% | -2% | -1% | 1% | 1% | -2% |
| 2014 CO ₂ Effective Radiative Forcing | | 3% | 8% | 14% | | | | | -1% | -2% | -1% | -1% | -1% | |
| 2014 Aerosol Effective Radiative Forcing | | -12% | -13% | -27% | | 44% | 29% | | -1% | -1% | -7% | -7% | -19% | |
| 2018 Ocean Heat Content rel. to 1971 | | | | | 51% | | | | 1% | 1% | 1% | 1% | 1% | |
| 2011 CH ₄ Effective Radiative Forcing | | 5% | -1% | -5% | | | | | -1% | -1% | -3% | -3% | -3% | |
| 2011 N ₂ O Effective Radiative Forcing | | 4% | -2% | -7% | | | | | 1% | 1% | 2% | 2% | 2% | |
| 2011 F-Gases Effective Radiative Forcing | | 3% | 5% | 7% | | | | | 1% | 1% | 1% | 1% | 1% | |
| Climate model | MCE-v1-2 | | | | OSCARv3.1 | | | | SCM4OPTv2.1 | | | | | |
| Assessed range | vll | ll | c | lu | vlu | vll | ll | c | lu | vll | ll | c | lu | vlu |
| 2000-2019 GMST rel. to 1961-1990 | -1% | | 3% | 3% | 3% | 2% | -9% | 2% | 0% | -8% | 4% | 10% | 6% | 28% |
| Equilibrium Climate Sensitivity | -24% | -22% | -22% | -23% | -26% | -15% | -14% | -15% | -14% | 13% | 4% | 12% | 6% | -3% |
| Transient Climate Response | 23% | 4% | -6% | -12% | -15% | -1% | -10% | -10% | -10% | 61% | 35% | 9% | 0% | -6% |
| Transient Climate Response to Emissions | 0% | -18% | -23% | -23% | -27% | -21% | -24% | -24% | -24% | | | | | |
| 2014 CO ₂ Effective Radiative Forcing | | -1% | -0% | 1% | | 6% | 0% | 0% | 0% | | | | | |
| 2014 Aerosol Effective Radiative Forcing | | 10% | 6% | -9% | | -21% | -1% | -1% | -1% | | | | | |
| 2018 Ocean Heat Content rel. to 1971 | | -1% | -0% | 1% | | -20% | 5% | 28% | 28% | | | | | |
| 2011 CH ₄ Effective Radiative Forcing | | -1% | -3% | -4% | | 5% | -17% | -32% | -32% | | | | | |
| 2011 N ₂ O Effective Radiative Forcing | | -1% | -0% | -1% | | 26% | 5% | -11% | -11% | | | | | |
| 2011 F-Gases Effective Radiative Forcing | | 0% | -0% | 0% | | 15% | 4% | -6% | -6% | | | | | |

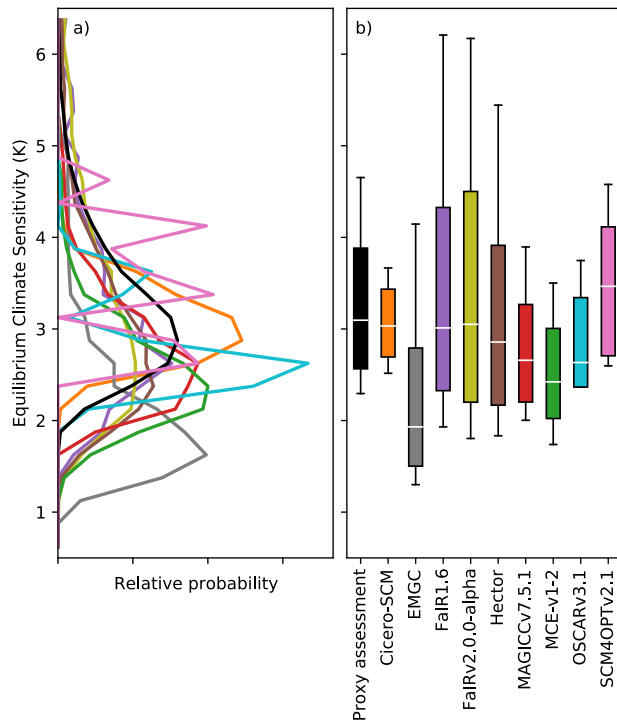


Figure 1. Distribution of Equilibrium Climate Sensitivity (ECS) from each RCM (coloured lines) and the proxy assessed range (solid black line). a) Distribution of ECS; b) Very likely (whiskers), likely (box) and central (white solid line) from the proxy assessment and each RCM.

379 median matches the very likely lower historical warming (rows labelled ‘2000-2019 GMST
 380 rel. to 1961-1990’ in Table 3) to within 7%. However, the multi-model median differs from
 381 the central and very likely upper historical warming by 11% and 25%, indicating that
 382 the models are having greater difficulty capturing the upper-end warming estimates.

383 There is also significant spread in performance across the models. MAGICCv7.5.1
 384 performs better than the multi-model median across all metrics and assessed ranges (very
 385 likely lower, likely lower, central, likely upper, very likely upper) except for ECS while
 386 MCE-v1-2 performs better than the multi-model median across all metrics and assessed
 387 ranges except for three metrics (ECS, TCR and TCRE). However, all RCMs had at least
 388 one metric where they matched the proxy assessment at all likelihood levels to within
 389 20% (bold cells in Table 3). For many applications, agreement to within 20% will be
 390 sufficient given the uncertainty associated with assessed ranges. However, for some ap-
 391 plications, using an RCM’s probabilistic distribution which has differences greater than
 392 5-10% (for certain metrics) may be problematic as such differences could bias projections
 393 to an unacceptably large degree. For example, the WG3 classification of scenarios in terms
 394 of their peak warming levels should ideally be consistent with the range of evidence as-
 395 sessed in IPCC WG1. To have confidence that such an application is reflecting the WG1
 396 assessment, the RCMs should be within 5-10% of the assessed results (particularly for
 397 any future warming assessment).

398 When interpreting these results it is vital to keep in mind that, for some models,
 399 the same benchmarks are used to both constrain and evaluate the models. The reason
 400 for this choice is that we are evaluating the ability of the models to act as integrators
 401 of knowledge i.e. to simultaneously capture all the independent assessments (see also dis-

402 cussion in Section 1). We are not attempting to do a calibration followed by an out-of-
 403 sample evaluation, instead we are looking at how well the RCMs can act as integrators
 404 of knowledge.

405 As a result, it is not so surprising that the models which calibrated to the bench-
 406 marks, specifically MAGICC7 and MCE-v1-2, better reflect the benchmarks during the
 407 evaluation phase. However, the results presented here highlight just how important it
 408 is to calibrate if the model is to be used as an integrator of knowledge. If the goal is an
 409 integrator of knowledge which reflects key benchmarks, our results suggest that mod-
 410 els which are calibrated will perform better.

411 4.2 Projection results

412 For each probabilistic setup, the RCMs also submitted projections of global-mean
 413 surface temperature, effective radiative forcing (split into total, aerosols and CO₂) and
 414 atmospheric CO₂ concentrations for the SSPX-Y.Y, ESM-SSPX-Y.Y and ESM-SSPX-
 415 Y.Y-allGHG experiments.

416 4.2.1 Global-mean Surface Air Temperature

417 Under SSP1-1.9, median end of century (2081-2100) projections relative to 1995-
 418 2014 vary by 0.4°C across the models (from Hector with 0.3°C of warming to SCM4OPTv2.1
 419 with 0.7°C, Figure 2 a)-c)). Variations in 5th percentile warming show a similar range,
 420 from 0.0°C to 0.4°C. In contrast, upper-end, 95th percentile warming shows far greater
 421 variation, from 0.8°C to 1.9°C. For the SSP1-1.9 scenario, the spread in RCMs' proba-
 422 bilistic projections is similar to the spread in the CMIP6 multi-model ensemble. Nonethe-
 423 less, the most extreme CMIP6 model projections are outside the range of most RCMs'
 424 5-95th percentiles. We discuss reasons for this difference in Section 4.3.

425 A slightly smaller spread is seen in peak temperature (Figure 2 f)-g)). Across the
 426 RCM ensemble, SSP1-1.9 median peak warming ranges from 0.55°C to 0.8°C while the
 427 5th and 95th percentiles range from 0.3°C to 0.7°C and 0.9°C to 2.0°C, respectively. The
 428 year of peak warming shows much more variation, particularly at the upper end (Fig-
 429 ure 2 d)-e)). While the median peak year is fairly consistent across the RCMs' ensem-
 430 bles, around 2045 (although SCM4OPTv2.1's 2055 peak is a clear outlier), and the 5th
 431 percentile peak year varies from 2030 to 2040, the 95th percentile varies from 2050 to be-
 432 yond the end of this century. In the EMGC, FaIR1.6 and FaIRv2.0.0-alpha probabilis-
 433 tic distributions, there is a significant area of parameter space which results in ongoing
 434 warming even after CO₂ emissions have reached net zero. These models also drive the
 435 spread in end of century temperature projections, particularly in the 95th percentile (Fig-
 436 ure 2 b)-c)).

437 In the SSP1-2.6 scenario (Supplementary Figure S10), median peak warming ranges
 438 from 0.65-1.1°C (0.1-0.3°C higher than in SSP1-1.9). Median end of century warming
 439 (relative to 1995-2014) ranges from 0.6°C to 1.0°C. End of century 5th percentile warm-
 440 ing ranges from 0.2°C to 0.8°C and 95th percentile warming ranges from 1.2°C to 2.0°C.
 441 As in SSP1-1.9, a number of CMIP6 model projections lie above the upper end of the
 442 constrained RCMs.

443 Under SSP1-2.6, the RCMs diverge more in their peak temperature projections,
 444 both compared to end of century warming and compared to SSP1-1.9. Once again, the
 445 5th percentile and median are fairly consistent (ranging from 0.3°C to 0.9°C and 0.65°C
 446 to 1.1°C respectively). However, 95th percentile projections vary from 1.2°C to 2.8°C.
 447 The divergence in upper-end warming between SSP1-2.6 and SSP1-1.9 is driven by FaIR1.6,
 448 and appears to be the result of persistent warming after CO₂ emissions reach net zero
 449 given that its 83rd percentile peak warming year is after 2100. Across the models, peak
 450 warming year shows a similar range to SSP1-1.9, albeit occurring 25-30 years later in the

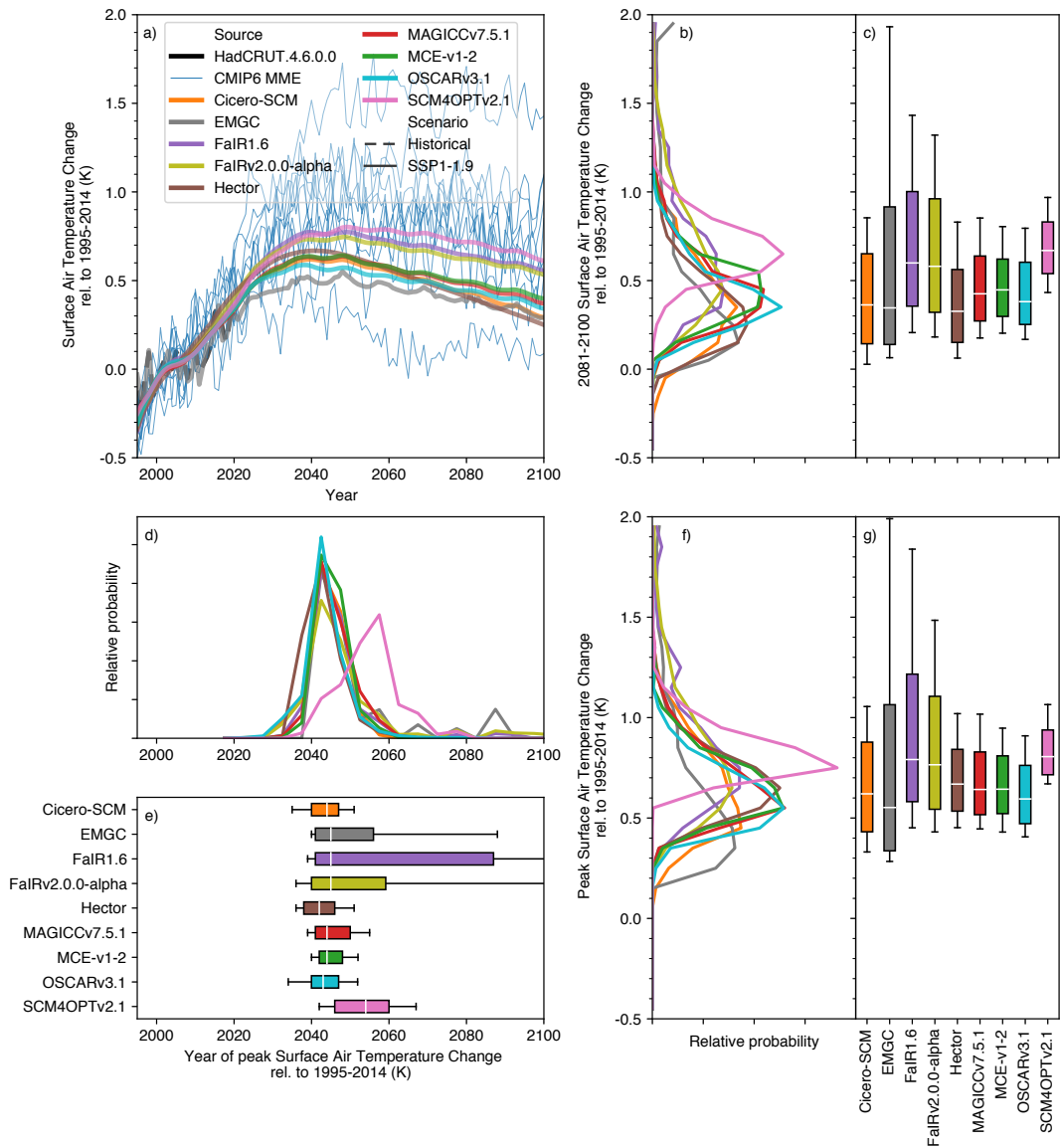


Figure 2. Surface air temperature (also referred to as global-mean surface air temperature, GSAT) change under the very low-emissions SSP1-1.9 scenario. a) GSAT projections from 1995 to 2100. We show the median RCM projections (coloured lines), GMST observations from HadCRUT4.6.0.0 (Morice et al., 2012) up to 2019 (dashed black line) and CMIP6 model projections (thin blue lines, we show a single ensemble member for each CMIP6 model to preserve the CMIP6 models' natural variability signal); b) distribution of 2081-2100 mean GSAT from each RCM; c) very likely (whiskers), likely (box) and central (white line) 2081-2100 mean GSAT estimate from each RCM; d) as in b) except for the year in which GSAT peaks; e) as in c) except for the year in which GSAT peaks; f) as in b) except for the peak GSAT; g) as in c) except for the peak GSAT. All results are shown relative to the 1995-2014 reference period.

451 median (ranging from 2065 to 2075). Once again, the 5th percentile (ranging from 2050
 452 to 2060) shows a much smaller spread across the models than the 95th percentile (rang-
 453 ing from 2075 to beyond the end of the 21st Century).

454 The warmest RCMs in mitigation scenarios are also the warmest under the high-
 455 emissions, SSP5-8.5, scenario (Supplementary Figure S11). The exceptions to this are
 456 MAGICC7, which is one of the warmest models in SSP5-8.5 even though it was around
 457 the median in mitigation scenarios, and SCM4OPTv2.1, which was the warmest model
 458 in mitigation scenarios but is slightly cooler than the warmest models in SSP5-8.5. Un-
 459 der SSP5-8.5, median end of century warming ranges from 2.5°C to 3.6°C across the RCMs.
 460 Unlike the mitigation scenarios, there is a similar level of disagreement in 5th and 95th
 461 percentile warming, with the 5th percentile ranging from 1.7°C to 3.1°C and the 95th per-
 462 centile ranging from 3.8°C to 5.4°C. The RCMs all make future warming projections in
 463 the lower-half of the CMIP6 multi-model ensemble. Such a difference is largely explained
 464 by the constraints applied to the RCMs (see discussion in Section 4.3).

465 If we consider long-term (2250-2300) warming under the SSP5-8.5 scenario (Fig-
 466 ure 3, see Supplementary Figure S12 and Supplementary Figure S13 for long-term warm-
 467 ing under SSP1-1.9 and SSP1-2.6 respectively), the difference between RCMs and CMIP6
 468 is even clearer (although the few CMIP6 models which have run the SSP5-8.5 extension
 469 are all at or above the median of the CMIP6 multi-model ensemble in 2100). On these
 470 timescales, MAGICC7 is clearly the warmest model, despite having slightly lower long-
 471 term effective radiative forcing than FaIR1.6, FaIR-v2.0.0-alpha and MCE-v1-2 (Sup-
 472 plementary Figure S14). There is a significant spread in long-term projections across the
 473 RCMs, with the median ranging from 4.5°C to 8.0°C, 5th percentile from 3°C (ignoring
 474 SCM4OPTv2.1 as an outlier) to 5.8°C and 95th from 7.8°C to 12.3°C. Even these up-
 475 per end projections are well below the highest CMIP6 projections, which reach over 16°C
 476 of global-mean warming (again, likely due to constraining, see discussion in Section 4.3).
 477 Across all the RCMs, only CICERO-SCM shows any sign of temperatures peaking by
 478 2300 under such a high-emissions scenario.

479 **4.2.2 Effective Radiative Forcing**

480 Compared to temperatures, there is less variance in end of century total effective
 481 radiative forcing projections (Figure 4, Supplementary Figure S15 and Supplementary
 482 Figure S16). This finding reinforces the understanding that the parameterisation of the
 483 climate response to effective radiative forcing is a key driver of climate projection un-
 484 certainty.

485 In SSP1-1.9, 2081-2100 mean total effective radiative forcing varies from 2.2 W /
 486 m² to 2.6 W / m². The 5th percentile ranges from 1.8 W / m² to 2.1 W / m² across the
 487 models (excluding CICERO-SCM which has an extremely narrow range). The spread
 488 is larger for the 95th percentile, which ranges from 2.4 W / m² to 3.2 W / m². This pat-
 489 tern, of uncertainty being higher for upper percentiles than lower percentiles, is seen across
 490 other key scenarios and highlights that the high-end effective radiative forcing projec-
 491 tions are much more uncertain than the best case and low-end effective radiative forc-
 492 ing projections.

493 In SSP1-2.6 (Supplementary Figure S15, once again excluding CICERO-SCM be-
 494 cause of its narrow range) median 2081-2100 total effective radiative forcing ranges from
 495 2.9 W / m² to 3.4 W / m² while the 5th percentile only ranges from 2.4 W / m² to 2.7
 496 W / m² and the 95th percentile has a much wider range of 3.1 W / m² to 4.1 W / m².
 497 Under SSP5-8.5 (Supplementary Figure S16, excluding EMGC and CICERO-SCM as
 498 outliers), median 2081-2100 total effective radiative forcing ranges from 8.0 W / m² to
 499 9.3 W / m² while the 5th percentile only ranges from 7.4 W / m² to 7.8 W / m² and the
 500 95th percentile has a much wider range of 8.4 W / m² to 11.0 W / m².

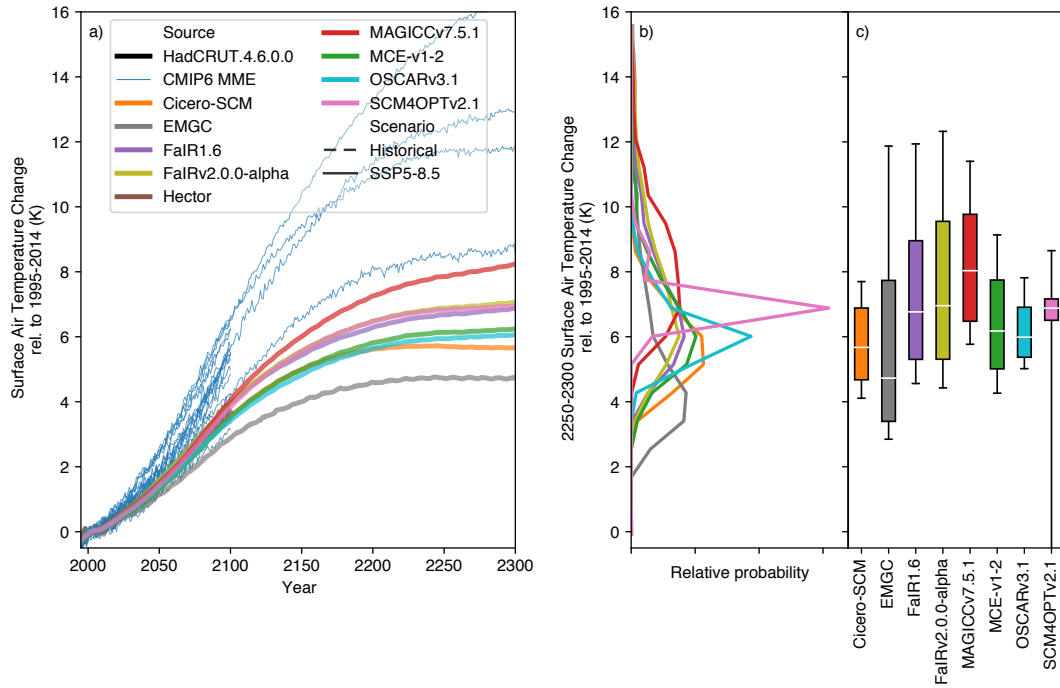


Figure 3. Long-term surface air temperature (also referred to as global-mean surface air temperature, GSAT) change under the high-emissions SSP5-8.5 scenario. a) GSAT projections from 1995 to 2300. We show the median RCM projections (coloured lines), GMST observations from (Morice et al., 2012) up to 2019 (dashed black line) and available CMIP6 model projections (thin blue lines, we show a single ensemble member for each CMIP6 models' natural variability signal); b) distribution of 2250-2300 mean GSAT from each RCM; c) very likely (whiskers), likely (box) and central (white line) 2250-2300 mean GSAT estimate from each RCM. All results are shown relative to the 1995-2014 reference period.

501 The approximate agreement in total effective radiative forcing is reflected in the
 502 agreement of each of the key contributors to this total, namely CO₂ and aerosol effective
 503 radiative forcing (Figure 5 and Supplementary Figures S17 - S29, which also show
 504 ERF output up to the year 2300). The key exceptions to this are SCM4OPTv2.1 and
 505 OSCARv3.1's aerosol effective radiative forcing. This negative aerosol forcing is driven
 506 by SCM4OPTv2.1 and OSCARv3.1's inclusion of a climate feedback on aerosol effective
 507 radiative forcing. The climate feedback makes their median end of century aerosol
 508 effective radiative forcing 0.3 - 0.8 W / m² more negative than other RCMs across the
 509 scenarios, although the effect is stronger in OSCARv3.1 than in SCM4OPTv2.1. The
 510 strong aerosol forcing is somewhat compensated by other forcing agents although both
 511 these models have long-term ERF which is at the low end of the RCM ensemble under
 512 SSP5-8.5 (Supplementary Figure S14). The different aerosol ERF parameterisations war-
 513 rant further attention, particularly because models without this aerosol ERF - climate
 514 feedback may be underestimating the spread in future temperature projections.

515 *4.2.3 Carbon Cycle*

516 Moving beyond effective radiative forcing and its temperature response, we con-
 517 sider the behaviour of the carbon cycle in the different RCMs. Clearly, the analysis pre-
 518 sented here covers only a limited subset of the full range of carbon cycle behaviour and
 519 metrics. The analysis is intended to highlight variance in carbon cycle behaviour across
 520 the RCMs, providing the motivation for a more detailed future analysis. We use the emissions-
 521 driven ESM-SSPX-Y.Y set of scenarios, in which emissions of CO₂ are prescribed and
 522 atmospheric CO₂ concentrations are allowed to freely evolve (in contrast to the SSP ex-
 523 periments in which CO₂ concentrations are prescribed).

524 There are considerable variations between the RCMs which submitted relevant re-
 525 sults (Supplementary Figure S30, Supplementary Figure S31 and Figure 6). In esm-SSP1-
 526 1.9 (Supplementary Figure S30, excluding CICERO-SCM because of its narrow range),
 527 the spread in median peak atmospheric CO₂ concentrations (430 ppm to 450 ppm) is
 528 similar to the spread in 2081-2100 median concentrations (385 ppm to 410 ppm). Sim-
 529 ilarly, in esm-SSP1-2.6 (Supplementary Figure S31, again excluding CICERO-SCM), the
 530 spread in median peak atmospheric CO₂ concentrations (450 ppm to 480 ppm) shows
 531 a spread similar to the spread in 2081-2100 median concentrations (430 ppm to 460 ppm).
 532 Under both scenarios, there are wide variances in percentile ranges across the models,
 533 with MAGICC7 showing the largest uncertainty in 2081-2100 atmospheric CO₂ concen-
 534 trations and SCM4OPTv2.1 showing the least (arguably, this model's range is overly con-
 535 fident). The considerable spread in projections from the models highlights the impor-
 536 tance of carbon cycle uncertainty for emissions-driven projections. The spread reinforces
 537 the need for a detailed study into available techniques for evaluating and potentially con-
 538 straining carbon cycle behaviour. Such a study would provide information about whether
 539 any of these projections can be ruled out based on other lines of evidence.

540 Next, we consider esm-SSP5-8.5, the only scenario with available CMIP6 Earth Sys-
 541 tem Model results (Figure 6). Median 2081-2100 atmospheric CO₂ concentrations range
 542 from 920 ppm to 1 000 ppm while 5th percentile and 95th percentile concentrations range
 543 from 800 ppm to 930 ppm and 910 ppm to 1 130 ppm respectively. MAGICC7 once again
 544 shows the largest uncertainties, but is more similar to the other RCMs than in the other
 545 scenarios. These comparisons highlight differences in the dynamics of the carbon cycle
 546 (and its feedbacks) in the various RCMs: uncertainties widen to a greater extent in higher-
 547 warming scenarios in FaIR1.6. FaIRv2.0.0-alpha, MCE-v1-2, OSCARv3.1 and SCM4OPTv2.1
 548 compared to MAGICC7.

549 Median atmospheric CO₂ projections from all of the RCMs lie within the plume
 550 of available CMIP6 results (Figure 6). FaIR1.6 lies at the top end of the CMIP6 plume,
 551 and its 5-95th range does not include low end CMIP6 results. In contrast, SCM4OPTv2.1

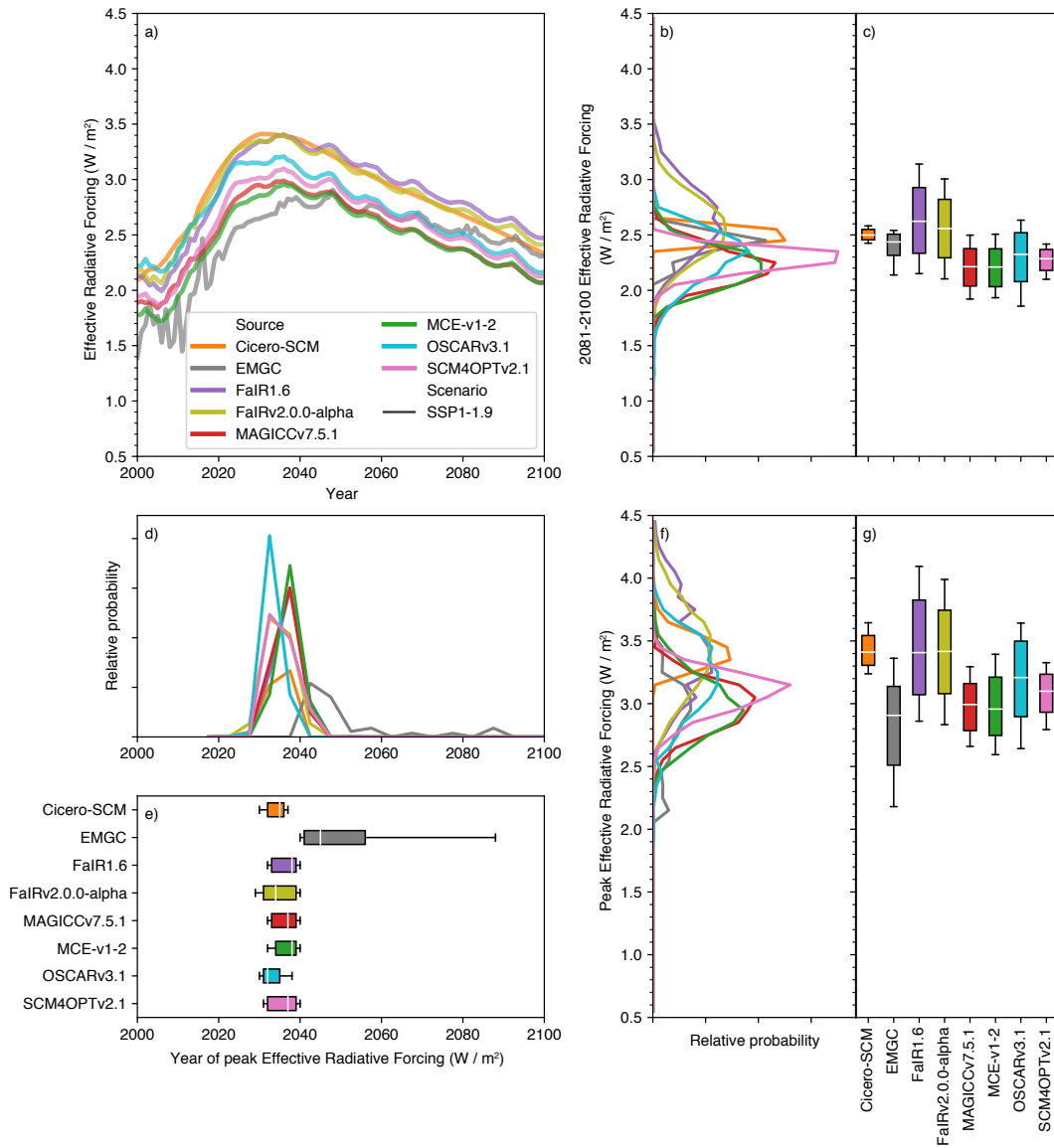


Figure 4. Effective radiative forcing under the very low-emissions SSP1-1.9 scenario. a) Median effective radiative forcing projections from 1995 to 2100 for each RCM; b) distribution of 2081-2100 mean effective radiative forcing from each RCM; c) very likely (whiskers), likely (box) and central (white line) 2081-2100 mean effective radiative forcing estimate from each RCM; d) as in b) except for the year in which effective radiative forcing peaks; e) as in c) except for the year in which effective radiative forcing peaks; f) as in b) except for the peak effective radiative forcing; g) as in c) except for the peak effective radiative forcing.

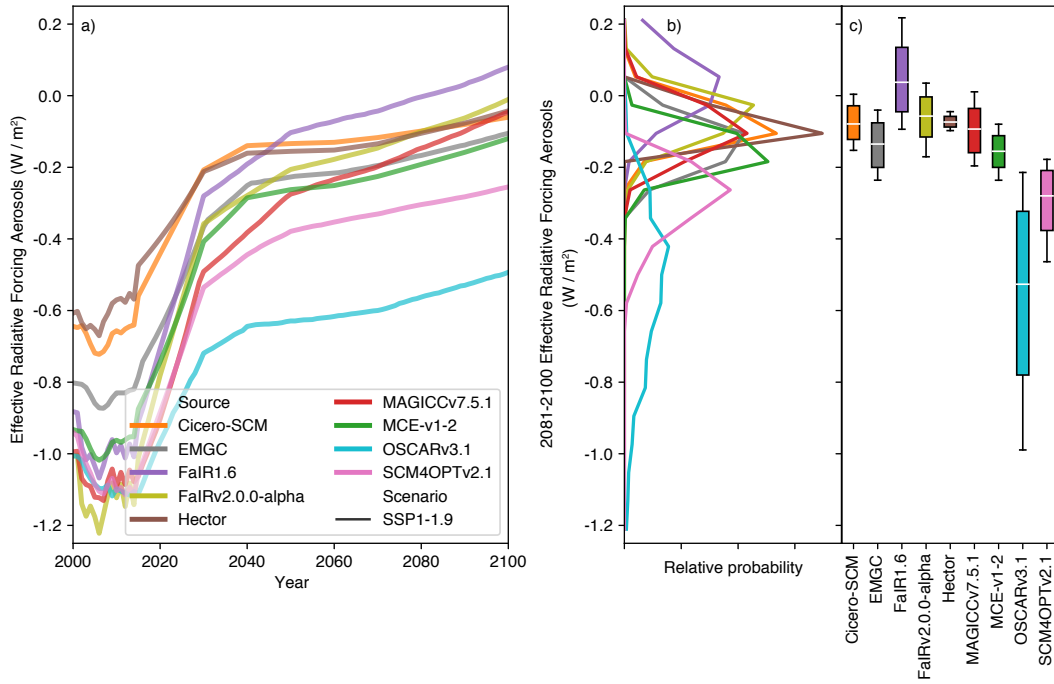


Figure 5. As in panels a), b) and c) of Figure 4, except for effective radiative forcing due to aerosols.

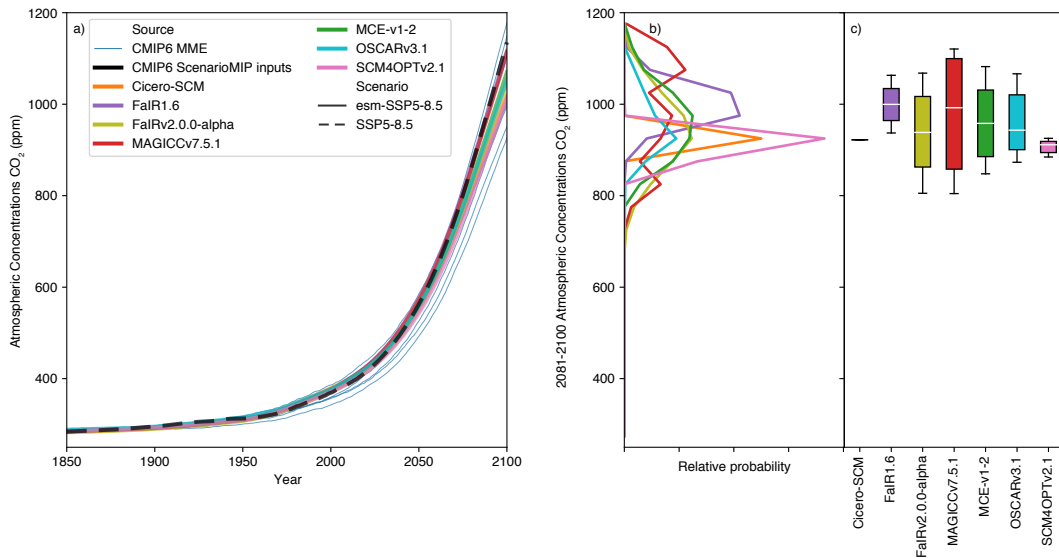


Figure 6. Atmospheric CO₂ concentration projections in the esm-SSP5-8.5 experiment. a) Atmospheric CO₂ concentration projections from 1995 to 2100. We show the median RCM projections (coloured lines), prescribed CMIP6 ScenarioMIP input concentrations from the SSP5-8.5 concentration-driven experiment (dashed black line) and available CMIP6 model projections (thin blue lines, we show a single ensemble member for each CMIP6 model to preserve the CMIP6 models' natural variability signal); b) distribution of 2081-2100 mean atmospheric CO₂ concentration projections from each RCM; c) very likely (whiskers), likely (box) and central (white line) 2081-2100 mean atmospheric CO₂ concentration projections estimate from each RCM. Note that FalR1.6 data is taken from the esm-SSP5-8.5-allGHG simulations because esm-SSP5-8.5 simulations are not available.

552 lies at the bottom end of the CMIP6 plume. FaIR-v2.0.0-alpha, MAGICC7, MCE-v1-
 553 2 and OSCARv3.1 approximately span the CMIP6 range, with FaIR-v2.0.0-alpha's and
 554 MCE-v1-2's ranges being almost exactly in line with the CMIP6 range whilst MAGICC7's
 555 projections are slightly wider than the CMIP6 range and OSCARv3.1's projections are
 556 slightly narrower than the CMIP6 range. CICERO-SCM does not include uncertainty
 557 in the carbon cycle, nor temperature feedbacks on the carbon cycle, hence produces only
 558 a single best-estimate projection.

559 Despite the limits of our carbon cycle evaluation, it is notable that the CMIP6 Sce-
 560 narioMIP input concentrations are generally higher than the RCMs' medians in emissions-
 561 driven runs across all considered scenarios. Emissions-driven scenario data from CMIP6
 562 ESMs is almost exclusively related to the esm-SSP5-8.5 experiment. Hence, while the
 563 pattern appears to be that the prescribed SSP5-8.5 CMIP6 concentrations are at the high-
 564 end of the range compared to the esm-SSP5-8.5 CMIP6 ESM results, there is little data
 565 with which to determine whether the prescribed CO₂ concentrations in the low-emissions
 566 scenarios would be within the projected concentration change by emission-driven ESM
 567 models. In hindsight, the input atmospheric CO₂ concentrations used in the concentration-
 568 driven runs may turn out to be at the high-end of CMIP6 ESM results across a range
 569 of scenarios. Given that only one set of input concentrations can be used in CMIP6, it
 570 is not surprising that the CO₂ concentrations prescribed for CMIP6 experiments do not
 571 sit exactly in the middle of later emissions-driven runs. The opposite was observed in
 572 CMIP5: the input CO₂ concentrations (derived with MAGICC6) were found to be in
 573 the lower-half of the CMIP5 emissions-driven runs that later emerged from the CMIP5
 574 emissions-driven runs (Friedlingstein et al., 2014). The CMIP6 concentrations were de-
 575 rived using an alpha version of MAGICC7, calibrated to approximately the median of
 576 the CMIP5 ESM carbon cycle responses with the inclusion of permafrost CO₂ and methane
 577 feedbacks (Meinshausen et al., 2020). Choosing a carbon cycle parameterisation more
 578 in line with the median of CMIP5 models appears to have lead to CO₂ concentrations
 579 which are now in the upper-half of CMIP6 ESM projections (Figure 6). Whenever a sin-
 580 gle estimate of the relationship between CO₂ emissions and concentrations is used, there
 581 is always the risk that it will not be the central estimate of the next generation of ESMs
 582 as our understanding of the carbon cycle improves and the ensembles of participating
 583 ESMs changes in each intercomparison phase. While this does not invalidate the design
 584 of concentration-driven experiments which are developed in this way, it must be kept in
 585 mind when relating emissions scenarios and the output of concentration-driven CMIP
 586 experiments.

587 *4.2.4 All greenhouse gas emissions-driven runs*

588 The final set of experiments we present are the experiments which are most rele-
 589 vant to WG3: all greenhouse gas emissions-driven runs. As discussed in Section 1, WG3
 590 describes scenarios in terms of their emissions hence needs models which can run in a
 591 fully-emissions driven setup. The cost of running ESMs for a large number of scenarios
 592 and parameter configurations in such a setup is computationally prohibitive (and few
 593 ESMs include key feedbacks such as methane permafrost and wetland emissions), hence
 594 there is a paucity of data against which to evaluate the projections of RCMs in such ex-
 595 periments. Nonetheless, here we present the results of such experiments in the hope that
 596 they will inspire further efforts into how to validate RCMs in this fully-coupled, all green-
 597 house gas emissions driven setup.

598 Five models (CICERO-SCM, FaIR1.6, FaIRv2.0.0-alpha, MAGICC7 and SCM4OPTv2.1)
 599 have submitted results for the all greenhouse gas emissions-driven scenarios. The results
 600 suggest that the all greenhouse gas emissions-driven runs are cooler and peak earlier than
 601 the concentration-driven runs (Figure 7, Supplementary Figure S32 and Supplementary
 602 Figure S33). However, the magnitude of the difference varies across the models. For median
 603 projections, MAGICC7 suggests the smallest difference between concentration-driven

604 and all greenhouse gas emissions-driven runs while CICERO-SCM and SCM4OPTv2.1
 605 imply differences of up to 0.3°C for peak and 2081-2100 warming and a peak in warm-
 606 ing up to ten years earlier. The range of projections in the all greenhouse gas emissions-
 607 driven runs are generally about the same or slightly wider than in the concentration-driven
 608 runs, with MAGICC7 showing the largest increase in projection ranges.

609 The lower-warming and wider projection ranges seen in all greenhouse gas emissions-
 610 driven runs are consistent with two other bits of knowledge. The first is that median CO₂
 611 concentrations are lower in all greenhouse gas emissions-driven runs than in concentration-
 612 driven runs (Section 4.2.3). The second is that carbon cycle and other greenhouse gas
 613 cycle uncertainties are included in temperature projections in all greenhouse gas emissions-
 614 driven runs, whilst these uncertainties are missing in concentration-driven runs. The dif-
 615 ference between the all greenhouse gas emissions-driven runs and concentration-driven
 616 runs reinforces the need for further consideration of RCM behaviour beyond the climate
 617 response to ERF.

618 4.3 Further Discussion

619 Our results prompt consideration of a number of further points. Firstly, the assess-
 620 ment performed here provides a way to easily identify differences between an RCM's be-
 621 haviour and the assessed range of a particular metric. Such differences are important to
 622 quantify, as they can reveal biases in a probabilistic distribution. The quantification makes
 623 it possible for the users of these distributions to identify where the biases might impact
 624 their own conclusions.

625 There are, however, cases where the issue lies in the combination of the proxy as-
 626 sessed ranges taken together, rather than in the probabilistic distributions. In this study,
 627 we used a combination of ECS from the literature (based on multiple lines of evidence),
 628 TCR from constrained CMIP6 models and TCRE from unconstrained CMIP6 Earth Sys-
 629 tem Models. This combination is likely to be slightly inconsistent. Unfortunately, incon-
 630 sistency between metric values is an inevitable risk of using independent lines of evidence.
 631 The potential inconsistency could in part explain our finding that the RCMs' TCR ranges
 632 are generally too high, while their ECS and TCRE ranges are generally too low. To ex-
 633 plain the inconsistency in more detail, firstly consider the ratio between TCR and ECS
 634 i.e. the realised warming fraction. The realised warming fraction implied by our TCR
 635 and ECS distributions is around 0.5. This is at the low end of the assessment by Millar
 636 et al. (2015). Hence, it can be argued that greater consistency within the proxy assess-
 637 ment would be achieved if either our proxy assessed TCR values were larger, or our proxy
 638 assessed ECS values were smaller. Similarly, the airborne fraction implied by our TCR
 639 and TCRE assessment is around 0.65. This is at the high-end of the CMIP5 and CMIP6
 640 range quantified by Arora et al. (2020). Once again, it can be argued that greater con-
 641 sistency within the proxy assessment would be achieved if either our proxy assessed TCR
 642 values were larger, or our proxy assessed TCRE values were smaller. Identifying such
 643 inconsistencies is a useful secondary benefit of exercises such as the one performed here.

644 Next, while they are a useful way of quickly visualising a model's agreement with
 645 the (here proxy) assessed ranges, summary tables of the form of Table 3 hide the full story.
 646 Specifically, for timeseries based variables, assessed ranges can only consider the trend
 647 or change between specific reference periods and don't consider the entire timeseries as
 648 a whole.

649 Not considering the entire timeseries can lead to problematic interpretations of the
 650 agreement between a model and the assessment. A clear example here is historical sur-
 651 face air ocean blended temperature change. In our proxy assessment, we focussed on 2000-
 652 2019 warming relative to the 1961-1990 reference period. On this measure, many of the
 653 RCMs were too warm compared to observations. However, the level of agreement is clearly
 654 reference period dependent (Figures 8a) and 8b)). In Figure 8a), which uses a 1961-1990

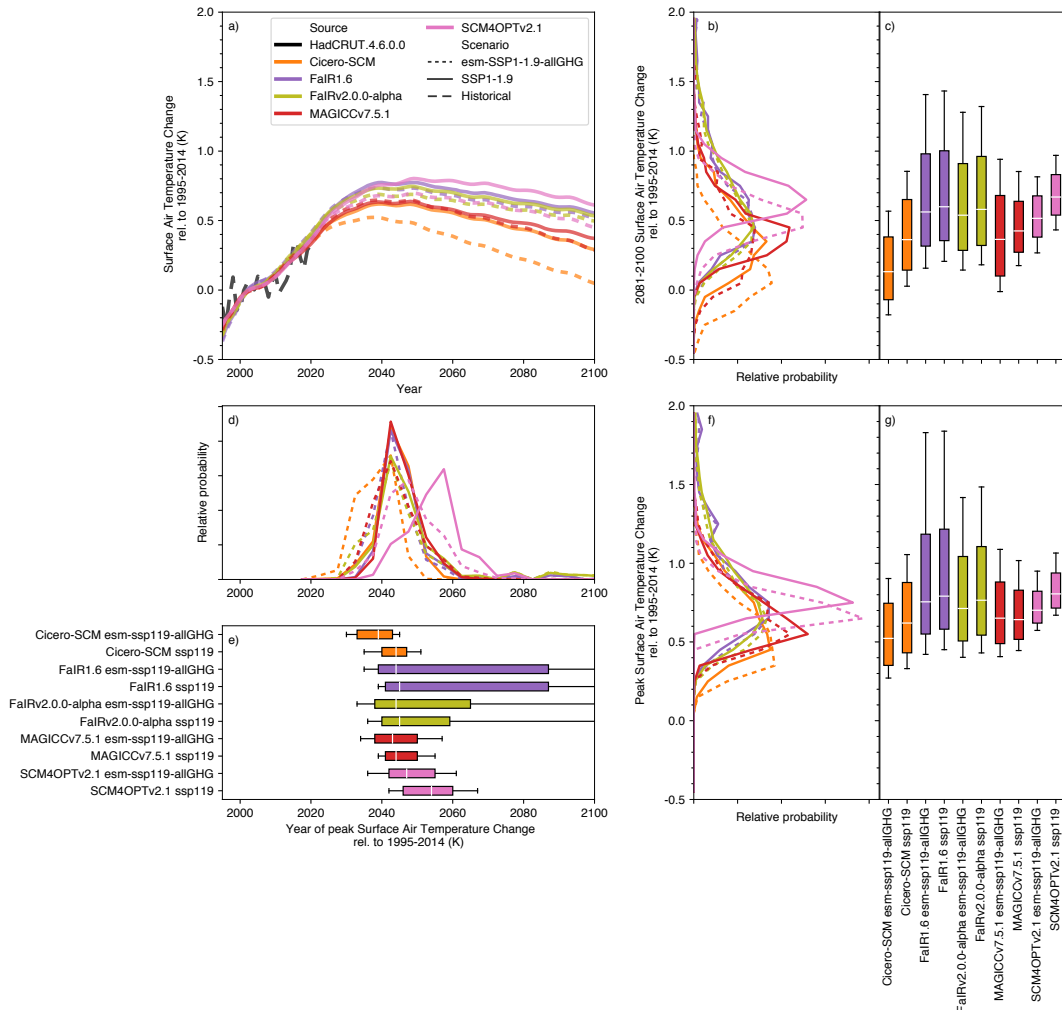


Figure 7. Surface air temperature (also referred to as global-mean surface air temperature, GSAT) change in the concentration-driven SSP1-1.9 experiment and the all greenhouse gas emissions driven esm-SSP1-1.9-allGHG experiment. a) GSAT projections from 1995 to 2100. We show the median RCM projections (coloured lines) for the concentration-driven experiment (solid) and all greenhouse gas emissions driven experiment (dashed) as well as observations up to 2019 (dashed black line); b) distribution of 2081-2100 mean GSAT for each scenario from each RCM; c) very likely (whiskers), likely (box) and central (white line) 2081-2100 mean GSAT estimate for each scenario from each RCM; d) as in b) except for the year in which GSAT peaks; e) as in c) except for the year in which GSAT peaks; f) as in b) except for the peak GSAT; g) as in c) except for the peak GSAT. All results are shown relative to the 1995-2014 reference period.

reference period, MAGICC7, MCE-v1-2 and OSCARv3.1 show the best agreement with observations (as also seen in Table 3). However, if we use a different reference period, e.g. 1850-1900 (Figure 8b)), that impression changes with Hector, MAGICC7, and OSCARv3.1 being the closest to observations in the recent period.

Considering the entire timeseries provides a more robust check on model behaviour. Fitting only to one evaluation and reference period can be achieved by slightly adjusting different model behaviour e.g. aerosol effective radiative forcing. However, if the entire timeseries are considered with multiple reference periods, such tuning quickly becomes impossible and the check provides detail into how well a model's dynamics are consistent with observations.

Moving away from evaluating the models, we find that higher historical warming, ECS and TCR values generally lead to higher warming projections (an intuitive result). Hector provides an exception to this pattern, with relatively low temperature projections, especially in SSP1-1.9, despite its relatively high historical warming and TCR.

In the strong mitigation scenarios (SSP1-1.9 and SSP1-2.6), there is agreement to within $\sim 0.1^\circ\text{C}$ in future projections (both best-estimate and range) between the models which best reflect historical warming (MAGICC7, MCE-v1-2 and OSCARv3.1). This agreement suggests that constraining greatly increases confidence in future projections. However, a limited set of models also provided probabilistic distributions that are constrained to match HadCRUT.5.0.1.0 (Morice et al., 2021), which is significantly warmer than the HadCRUT.4.6.0.0 based constrained used in the rest of the study. The future projections from these HadCRUT.5.0.1.0-constrained distributions are noticeably warmer (Supplementary Figures S34 - S36) than projections from HadCRUT.4.6.0.0-constrained distributions, which demonstrates that projections are sensitive to the choice of constraint.

Given the sensitivity of conclusions to the constraint, the use of constraints must be carefully considered as it could lead to overconfidence (Sanderson et al., 2017). Even though considerable care is taken both here and elsewhere to identify and use relevant, physically justifiable, constraints, it is still possible that future research may show that the constraints are leading to overconfident future projections. Having said this, Herger et al. (2019) suggest that using multiple constraints, as is done by many RCMs here, reduces the likelihood of overconfidence.

Studies which constrain the raw CMIP6 model ensemble help explain the difference between the RCM-based results presented here and the raw CMIP6 model ensemble. Brunner et al. (2020), Liang et al. (2020) and Tokarska et al. (2020) all find significant reductions in both the best-estimate and 5-95% range GSAT projections after applying observed-warming constraints to the CMIP6 model ensemble. For the SSP1-2.6 and SS5-8.5 scenarios respectively, these studies find 5-95% GSAT (relative to 1995-2014) ranges of: Tokarska et al. (2020): $0.41\text{-}1.46^\circ\text{C}$ and $2.26\text{-}4.60^\circ\text{C}$; Liang et al. (2020) $0.52\text{-}1.66^\circ\text{C}$ and $2.72\text{-}4.77^\circ\text{C}$ and Brunner et al. (2020) $0.61\text{-}1.85^\circ\text{C}$ and $2.72\text{-}4.86^\circ\text{C}$. These estimates, particularly for the SSP1-2.6 scenario, are slightly wider than our results based on RCMs. However, the constrained CMIP6 estimates are much closer to our RCM-based estimates than the raw CMIP6 model ensemble, in particular for the 95th percentile. This suggests that the majority of the difference between our RCM-based results and the raw CMIP6 model ensemble is explained by the constraining applied to the RCMs, rather than structural differences between RCMs and CMIP6 models (although structural differences may explain the disagreement between constrained CMIP6 output and our results). Further studies are needed to explore the validity of the constraining approaches for both ESMs and RCMs - as investigated here - but this study lays the foundation for systematically investigating probabilistic RCM ensembles in more detail.

Given the proxy assessment and results, we make one final observation: to extrapolate assessed warming ranges from one set of scenarios (e.g. the RCP or SSP-based sce-

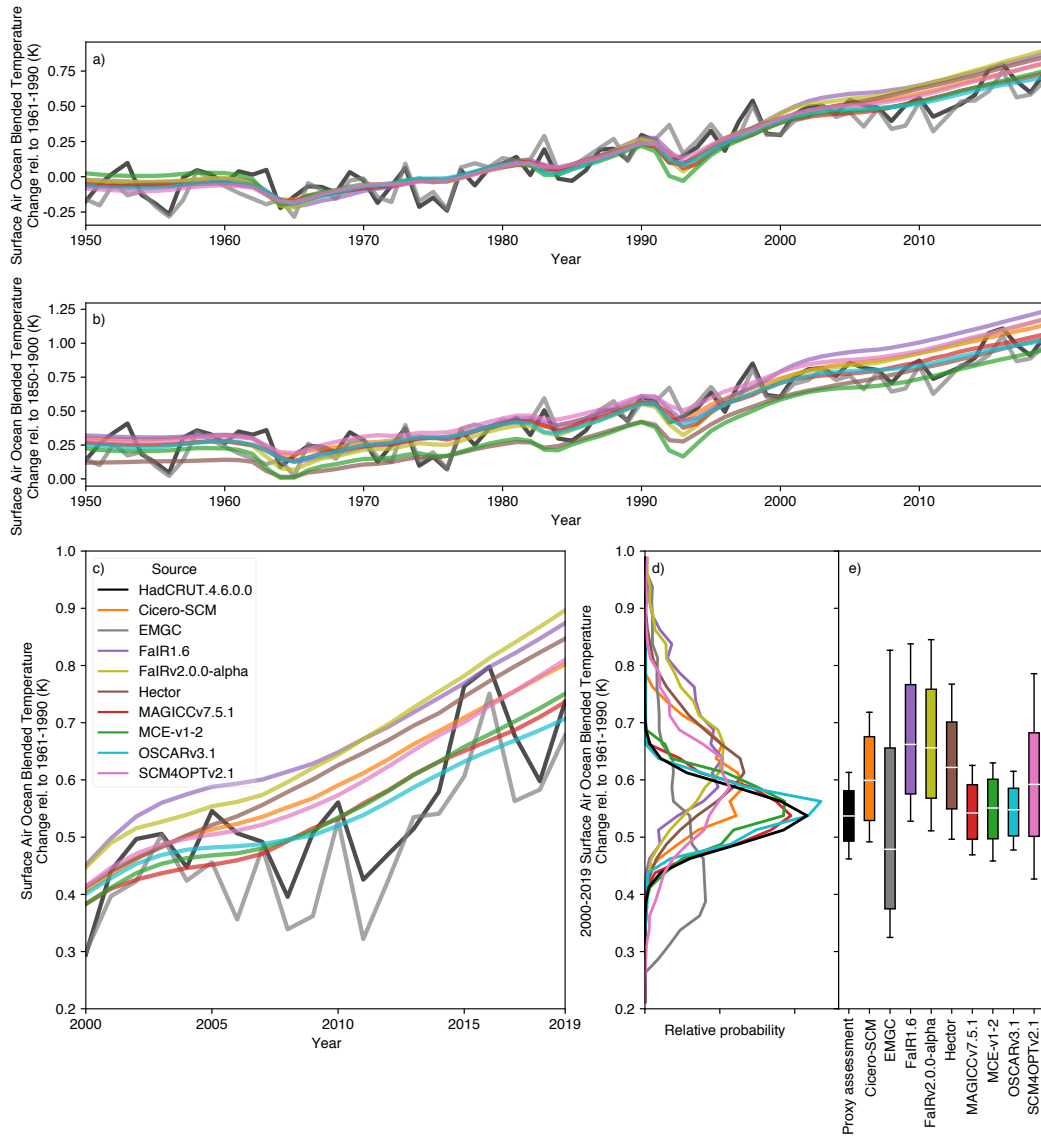


Figure 8. Historical surface air ocean blended temperature change (also referred to as global-mean surface temperature, GMST) from each RCM. We compare observations from HadCRUT4.6.0.0 (Morice et al., 2012) (solid black line) to the distribution from each RCM (coloured lines). All panels use 1961-1990 as the reference period, the same reference period as is used in our proxy assessed ranges, except b) which uses 1850-1900. a), b) median GMST from 1950 to 2019; c) median GMST from 2000 to 2019 (the proxy assessment period); d) distribution of 2000-2019 mean GMST from each RCM and the proxy assessed range; e) Very likely (whiskers), likely (box) and central (white line) estimate of 2000-2019 mean GMST from each RCM and the proxy assessed range. The historical simulation has been extended with SSP2-4.5 for the period 2015-2019.

narios) to a wider set of scenarios, it may be beneficial to include a benchmark of assessed future warming under the benchmark scenarios. This benchmark could be taken from other studies, e.g. those that constrain CMIP projections (for the limited number of scenarios run by CMIP) based on historical observations (e.g. Brunner et al., 2020; Liang et al., 2020; Tokarska et al., 2020). Adding such a benchmark to the historical observations, present-day assessments and idealised metrics used in this study would highlight where future warming significantly diverges from other lines of evidence. Including scenarios with similar end of century total ERF but different transient evolutions (like the SSP4-3.4 and SSP5-3.4-overshoot scenario pair) would provide an even stronger check of the models' transient response. Such quantifications could be key when assessing future projections under large sets of scenarios, like the WG3 scenario database climate assessment. Of course, the risk of adding such benchmarks is an artificial narrowing of uncertainty in projected warming. Hence, future projections should only be included where there is a clear need and justification for consistency between the RCMs' projections and the projections from other lines of evidence.

5 Future work

This exercise is a first step towards more comprehensive, routine evaluation of RCMs' probabilistic parameter ensembles and their corresponding projections. However, there is still much room for future work to improve on this study and the first phase of RCMIP. As a first suggestion, repeating this exercise with the assessed ranges from Working Group 1 of the Intergovernmental Panel on Climate Change's Sixth Assessment Report (due in mid 2021) would provide an evaluation of the extent to which RCMs can capture the latest international assessment of the scientific literature.

This future work could go beyond evaluation and also diagnose the root causes of differences between the models. One obvious area for examination would be the aerosol ERF, particularly the inclusion of a climate feedback in aerosol ERF parameterisations. Such an exercise could also provide greater insights into differences between the constrained RCMs' probabilistic distributions, the raw CMIP6 multi-model ensemble and constrained CMIP6 output (building on the discussion in Section 4.3).

A clear limitation of this study is the relative lack of examination of carbon cycle behaviour and carbon cycle related metrics. Given the importance of the carbon cycle for emissions-driven projections, this is another clear area for future work. In the limited examination we have performed, we chose to focus on emissions-driven simulations. This choice provides the cleanest comparison between RCMs and CMIP6 models, given that many RCMs do not separate the land and ocean carbon pools, although it limits us to a relatively small set of CMIP6-comparison data (given that only few emissions-driven simulations (Jones et al., 2016) have been run by CMIP6 models). An increase in the number of emissions-driven CMIP6 ESM model output, particularly for mitigation scenarios, would greatly aid such evaluations. Using the concentration-driven simulations in future work will also provide a greater set of comparison data and will facilitate evaluation of RCMs' land and ocean carbon cycles under more varied scenarios.

Finally, given how RCMs are typically used by WG3, it appears that a truly thorough evaluation would need to consider a larger set of individual steps in the emissions-climate change cause-effect chain. Such an evaluation would provide insights into the drivers of differences between future projections based on the concentration-driven experiments typical of CMIP and results based on the all greenhouse gas emissions-driven experiments required by WG3. While it is not completely clear to us which components would need to be considered (and which could be ignored), a first suggestion of important components is: the carbon cycle, other earth system feedbacks e.g. representation of permafrost, representation of aerosols, non-CO₂ greenhouse gas cycles, translation between changes in greenhouse gas concentrations and effective radiative forcing, ozone representation,

757 land-use change albedo representation, temperature response to effective radiative forc-
758 ing and all the feedbacks and interactions. To see the full picture, a broad range of lit-
759 erature would need to be considered as a validation source and a wide range of exper-
760 iments, spanning historical, scenario-based and idealised experiments, would need to be
761 performed. In performing a more thorough evaluation, an updated evaluation technique
762 may be required. Specifically, using percentage differences from the assessed range will
763 lead to problems when the assessed range is close to or spans zero. Hence, more sophis-
764 ticated ways of evaluating the agreement between model results and assessed ranges may
765 be required. For reasons of scope, we haven't achieved such a thorough evaluation here,
766 but we hope that this work provides a basis upon which future work can aim for the lofty
767 goal of more complete evaluation of all of the relevant parts of the climate system.

768 6 Conclusions

769 We have found that the best performing RCMs can match our proxy assessment
770 across a range of climate metrics. However, no RCM matched the proxy assessment across
771 all metrics. At the same time, all RCMs matched the proxy assessment well for at least
772 one metric.

773 Our evaluation is the first multi-model comparison of probabilistic projections from
774 RCMs. This exercise provides a unique insight into RCMs probabilistic parameter en-
775 sembles, specifically how they compare with a set of proxy assessed ranges, which reflect
776 wider scientific understanding of key climate metrics, and the implications of differences
777 in probabilistic distributions for climate projections across a range of climate variables
778 and scenarios.

779 Notably, although unsurprisingly, we found that models whose probabilistic dis-
780 tribution were constrained to the proxy assessed ranges were better able to reflect the
781 proxy assessed ranges. This point is notable because it makes clear that if RCMs are to
782 be used as integrators of knowledge, conveying multiple lines of evidence from one do-
783 main to another (e.g. IPCC WG1 to IPCC WG3), then RCMs whose probabilistic dis-
784 tributions have been constrained to the intended lines of evidence are likely to be the
785 best tool.

786 Even amongst models which had similar levels of agreement with the proxy assess-
787 ment, some divergence in future projections was observed. Given the various model struc-
788 tures that the reduced complexity models employ, ranging from linearised impulse re-
789 sponse functions to 50-layer ocean models, it is not surprising that models may diverge
790 in scenarios that go significantly beyond the domain of the validation data. Adding con-
791 straints on future performance i.e. extending the domain of validation data (for exam-
792 ple based on an independent assessment of warming in a limited subset of scenarios) would
793 likely reduce the divergence, although such extra constraints should be carefully consid-
794 ered given that they risk artificially narrowing projection uncertainty.

795 While exercises such as the one performed here can provide helpful information about
796 where the biases may lie, they cannot provide definitive answers about what the future
797 holds. It is possible to make judgements about what is more reasonable based on the eval-
798 uation performed here, and to rule out clearly incorrect projections, yet it must be recog-
799 nised that a definitive answer is impossible: we will not know which projections are cor-
800 rect until we get there, by which time it is too late for climate policy. Hence, while it
801 is important to continue to evaluate and improve our models to remove as many sources
802 of error as possible, it is also important that research into decision making under uncer-
803 tainty (e.g. Weaver et al., 2013; Dittrich et al., 2016) continues to develop and be used
804 because the uncertainty in projections will not disappear anytime soon, never in fact.
805 In addition, those who use RCMs for climate projections should carefully consider how

806 they're going to use the RCMs and how they're going to validate them before making
807 conclusions about the implications of their projections.

808 In addition, we found that many of the RCMs did not reproduce the high warming
809 seen in CMIP6 models. However, studies which constrain CMIP6 models based on
810 observational constraints also exclude such high warming which suggests that the lack
811 of high warming is due to the constraining applied to the RCMs, rather than structural
812 differences between RCMs and CMIP6 models. Beyond the question of temperature pro-
813 jections, we found that the prescribed CO₂ concentrations used in the CMIP6 SSP-based
814 experiments are at the high-end of projections made with historically constrained car-
815 bon cycles. Although, further investigations into carbon cycle behaviour are required to
816 provide a clearer picture of the influence of carbon cycle uncertainties on emissions-driven
817 projections. Finally, we observed that a change in reference period significantly altered
818 how well some models agreed with observations, reinforcing the need to consider more
819 than one reference period when evaluating models.

820 With sufficient validations, RCMs provide a unique synthesis tool to integrate the
821 latest scientific understanding, including its uncertainties, along the complex cause-effect
822 chain from emissions to global-mean temperatures. Integrating this understanding in an
823 internally consistent RCM framework, with all the implicit cross-correlations, is our best
824 method to inform decision-making and other scientific domains, for example the likeli-
825 hood of exceeding a given global-mean temperature threshold under a specific emissions
826 scenario. Further developing these tools opens vast opportunities to go beyond global-
827 mean variables and temperature changes, and to robustly represent the complex science
828 beneath.

829 Acknowledgments

830 Data and code to produce all the figures and tables can be obtained from [https://](https://doi.org/10.5281/zenodo.4269711)
831 doi.org/10.5281/zenodo.4269711.

832 ZN benefited from support provided by the ARC Centre of Excellence for Climate
833 Extremes (CE170100023).

834 KD's, DW's, AS's, SJS's and BVW's participation was supported by the U.S. De-
835 partment of Energy, Office of Science, as part of research in MultiSector Dynamics, Earth
836 and Environmental System Modeling Program.

837 CJS was supported by a NERC/IIASA Collaborative Research Fellowship (NE/T009381/1).
838

839 References

- 840 Arora, V. K., Katavouta, A., Williams, R. G., Jones, C. D., Brovkin, V., Friedling-
841 stein, P., ... Ziehn, T. (2020). Carbon-concentration and carbon-climate
842 feedbacks in cmip6 models and their comparison to cmip5 models. *Biogeo-*
843 *sciences*, 17(16), 4173–4222. Retrieved from [https://bg.copernicus.org/](https://bg.copernicus.org/articles/17/4173/2020/)
844 [articles/17/4173/2020/](https://bg.copernicus.org/articles/17/4173/2020/) doi: 10.5194/bg-17-4173-2020
- 845 Brunner, L., Pendergrass, A. G., Lehner, F., Merrifield, A. L., Lorenz, R., & Knutti,
846 R. (2020). Reduced global warming from cmip6 projections when weighting
847 models by performance and independence. *Earth System Dynamics Discus-*
848 *sions*, 2020, 1–23. Retrieved from [https://esd.copernicus.org/preprints/](https://esd.copernicus.org/preprints/esd-2020-23/)
849 [esd-2020-23/](https://esd.copernicus.org/preprints/esd-2020-23/) doi: 10.5194/esd-2020-23
- 850 Canty, T., Mascioli, N. R., Smarte, M. D., & Salawitch, R. J. (2013). An empirical
851 model of global climate – part 1: A critical evaluation of volcanic cooling. *At-*
852 *mospheric Chemistry and Physics*, 13(8), 3997–4031. Retrieved from <https://>

- 853 www.atmos-chem-phys.net/13/3997/2013/ doi: 10.5194/acp-13-3997-2013
- 854 Clarke, L., Jiang, K., Akimoto, K., Babiker, M., Blanford, G., Fisher-Vanden, K.,
855 ... et al. (2014). Assessing transformation pathways. In O. Edenhofer et al.
856 (Eds.), *Climate change 2014: Mitigation of climate change. contribution of*
857 *working group iii to the fifth assessment report of the intergovernmental panel*
858 *on climate change* (p. 413–510). Cambridge University Press.
- 859 Dittrich, R., Wreford, A., & Moran, D. (2016). A survey of decision-making
860 approaches for climate change adaptation: Are robust methods the way
861 forward? *Ecological Economics*, 122, 79 - 89. Retrieved from [http://](http://www.sciencedirect.com/science/article/pii/S0921800915004887)
862 www.sciencedirect.com/science/article/pii/S0921800915004887 doi:
863 <https://doi.org/10.1016/j.ecolecon.2015.12.006>
- 864 Etminan, M., Myhre, G., Highwood, E. J., & Shine, K. P. (2016, dec). Radiative
865 forcing of carbon dioxide, methane, and nitrous oxide: A significant revision of
866 the methane radiative forcing. *Geophysical Research Letters*, 43(24), 12,614–
867 12,623. doi: 10.1002/2016gl071930
- 868 Eyring, V., Bony, S., Meehl, G. A., Senior, C. A., Stevens, B., Stouffer, R. J., &
869 Taylor, K. E. (2016). Overview of the coupled model intercomparison project
870 phase 6 (cmip6) experimental design and organization. *Geoscientific Model*
871 *Development (Online)*, 9(LLNL-JRNL-736881).
- 872 Forster, P. M., Richardson, T., Maycock, A. C., Smith, C. J., Samset, B. H., Myhre,
873 G., ... Schulz, M. (2016). Recommendations for diagnosing effective ra-
874 diative forcing from climate models for cmip6. *Journal of Geophysical Re-*
875 *search: Atmospheres*, 121(20), 12,460-12,475. Retrieved from [https://](https://agupubs.onlinelibrary.wiley.com/doi/abs/10.1002/2016JD025320)
876 agupubs.onlinelibrary.wiley.com/doi/abs/10.1002/2016JD025320 doi:
877 10.1002/2016JD025320
- 878 Friedlingstein, P., Meinshausen, M., Arora, V. K., Jones, C. D., Anav, A., Lid-
879 dicoat, S. K., & Knutti, R. (2014, 01). Uncertainties in CMIP5 Climate
880 Projections due to Carbon Cycle Feedbacks. *Journal of Climate*, 27(2), 511-
881 526. Retrieved from <https://doi.org/10.1175/JCLI-D-12-00579.1> doi:
882 10.1175/JCLI-D-12-00579.1
- 883 Gasser, T., Ciais, P., Boucher, O., Quilcaille, Y., Tortora, M., Bopp, L., & Hauglus-
884 taine, D. (2017). The compact earth system model oscar v2.2: description
885 and first results. *Geoscientific Model Development*, 10(1), 271–319. Re-
886 trieved from <https://gmd.copernicus.org/articles/10/271/2017/> doi:
887 10.5194/gmd-10-271-2017
- 888 Gasser, T., Crepin, L., Quilcaille, Y., Houghton, R. A., Ciais, P., & Obersteiner,
889 M. (2020). Historical co2 emissions from land use and land cover change
890 and their uncertainty. *Biogeosciences*, 17(15), 4075–4101. Retrieved
891 from <https://bg.copernicus.org/articles/17/4075/2020/> doi:
892 10.5194/bg-17-4075-2020
- 893 Gasser, T., Kechiar, M., Ciais, P., Burke, E. J., Kleinen, T., Zhu, D., ... Ober-
894 steiner, M. (2018, Nov 01). Path-dependent reductions in co2 emission
895 budgets caused by permafrost carbon release. *Nature Geoscience*, 11(11),
896 830-835. Retrieved from <https://doi.org/10.1038/s41561-018-0227-0> doi:
897 10.1038/s41561-018-0227-0
- 898 Harmsen, M. J. H. M., van Vuuren, D. P., van den Berg, M., Hof, A. F., Hope, C.,
899 Krey, V., ... Schaeffer, M. (2015, sep). How well do integrated assessment
900 models represent non-CO2 radiative forcing? *Climatic Change*, 133(4), 565–
901 582. doi: 10.1007/s10584-015-1485-0
- 902 Haustein, K., Allen, M. R., Forster, P. M., Otto, F. E. L., Mitchell, D. M.,
903 Matthews, H. D., & Frame, D. J. (2017, Nov 13). A real-time global warming
904 index. *Scientific Reports*, 7(1), 15417. Retrieved from [https://doi.org/](https://doi.org/10.1038/s41598-017-14828-5)
905 [10.1038/s41598-017-14828-5](https://doi.org/10.1038/s41598-017-14828-5) doi: 10.1038/s41598-017-14828-5
- 906 Herger, N., Abramowitz, G., Sherwood, S., Knutti, R., Angélil, O., & Sisson, S. A.
907 (2019). Ensemble optimisation, multiple constraints and overconfidence: a case

- 908 study with future Australian precipitation change. *Climate Dynamics*, 53(3),
 909 1581–1596. Retrieved from <https://doi.org/10.1007/s00382-019-04690-8>
 910 doi: 10.1007/s00382-019-04690-8
- 911 Hooss, G., Voss, R., Hasselmann, K., Maier-Reimer, E., & Joos, F. (2001, dec). A
 912 nonlinear impulse response model of the coupled carbon cycle-climate system
 913 (NICCS). *Climate Dynamics*, 18(3-4), 189–202. doi: 10.1007/s003820100170
- 914 Hope, A. P., Canty, T. P., Salawitch, R. J., Tribett, W. R., & Bennett, B. F. (2017).
 915 Forecasting global warming [Book Section]. In *Paris climate agreement: Bea-*
 916 *con of hope* (p. 51-114). Springer Climate.
- 917 Hope, A. P., McBride, L. A., Canty, T. P., Bennett, B. F., Tribett, W. R., &
 918 Salawitch, R. J. (2020). Examining the human influence on global cli-
 919 mate using an empirical model. *Earth and Space Science Open Archive*,
 920 79. Retrieved from <https://doi.org/10.1002/essoar.10504179.1> doi:
 921 10.1002/essoar.10504179.1
- 922 Huppmann, D., Rogelj, J., Kriegler, E., Krey, V., & Riahi, K. (2018). A new sce-
 923 nario resource for integrated 1.5 °c research. *Nature Climate Change*, 8(12),
 924 1027–1030. doi: 10.1038/s41558-018-0317-4
- 925 Jones, C. D., Arora, V., Friedlingstein, P., Bopp, L., Brovkin, V., Dunne, J., ...
 926 Zaehle, S. (2016). C4mip – the coupled climate–carbon cycle model intercom-
 927 parison project: experimental protocol for cmip6. *Geoscientific Model Devel-*
 928 *opment*, 9(8), 2853–2880. Retrieved from [https://gmd.copernicus.org/](https://gmd.copernicus.org/articles/9/2853/2016/)
 929 [articles/9/2853/2016/](https://gmd.copernicus.org/articles/9/2853/2016/) doi: 10.5194/gmd-9-2853-2016
- 930 Joos, F., Bruno, M., Fink, R., Siegenthaler, U., Stocker, T. F., Quéré, C. L., &
 931 Sarmiento, J. L. (1996). An efficient and accurate representation of complex
 932 oceanic and biospheric models of anthropogenic carbon uptake. *Tellus B:*
 933 *Chemical and Physical Meteorology*, 48(3), 394-417. Retrieved from [https://](https://doi.org/10.3402/tellusb.v48i3.15921)
 934 doi.org/10.3402/tellusb.v48i3.15921 doi: 10.3402/tellusb.v48i3.15921
- 935 Kawamiya, M., Hajima, T., Tachiiri, K., Watanabe, S., & Yokohata, T. (2020).
 936 Two decades of Earth system modeling with an emphasis on Model for
 937 Interdisciplinary Research on Climate (MIROC). *Progress in Earth and*
 938 *Planetary Science*, 7(1), 64. Retrieved from [https://doi.org/10.1186/](https://doi.org/10.1186/s40645-020-00369-5)
 939 [s40645-020-00369-5](https://doi.org/10.1186/s40645-020-00369-5) doi: 10.1186/s40645-020-00369-5
- 940 Leach, N. J., Jenkins, S., Nicholls, Z., Smith, C. J., Lynch, J., Cain, M., ... Allen,
 941 M. R. (2020). Fairv2.0.0: a generalised impulse-response model for climate
 942 uncertainty and future scenario exploration. *Geoscientific Model Development*
 943 *Discussions*, 2020, 1–48. Retrieved from [https://gmd.copernicus.org/](https://gmd.copernicus.org/preprints/gmd-2020-390/)
 944 [preprints/gmd-2020-390/](https://gmd.copernicus.org/preprints/gmd-2020-390/) doi: 10.5194/gmd-2020-390
- 945 Liang, Y., Gillett, N. P., & Monahan, A. H. (2020). Climate model projections
 946 of 21st century global warming constrained using the observed warming
 947 trend. *Geophysical Research Letters*, 47(12), e2019GL086757. Retrieved
 948 from [https://agupubs.onlinelibrary.wiley.com/doi/abs/10.1029/](https://agupubs.onlinelibrary.wiley.com/doi/abs/10.1029/2019GL086757)
 949 [2019GL086757](https://agupubs.onlinelibrary.wiley.com/doi/abs/10.1029/2019GL086757) (e2019GL086757 2019GL086757) doi: [https://doi.org/10.1029/](https://doi.org/10.1029/2019GL086757)
 950 [2019GL086757](https://doi.org/10.1029/2019GL086757)
- 951 McBride, L. A., Hope, A. P., Canty, T. P., Bennett, B. F., Tribett, W. R., &
 952 Salawitch, R. J. (2020). Comparison of cmip6 historical climate sim-
 953 ulations and future projected warming to an empirical model of global
 954 climate. *Earth System Dynamics Discussions*, 2020, 1–59. Retrieved
 955 from <https://esd.copernicus.org/preprints/esd-2020-67/> doi:
 956 10.5194/esd-2020-67
- 957 Meinshausen, M., Meinshausen, N., Hare, W., Raper, S. C. B., Frieler, K., Knutti,
 958 R., ... Allen, M. R. (2009, Apr 01). Greenhouse-gas emission targets for lim-
 959 iting global warming to 2 °c. *Nature*, 458(7242), 1158-1162. Retrieved from
 960 <https://doi.org/10.1038/nature08017> doi: 10.1038/nature08017
- 961 Meinshausen, M., Nicholls, Z. R. J., Lewis, J., Gidden, M. J., Vogel, E., Freund, M.,
 962 ... Wang, R. H. J. (2020). The shared socio-economic pathway (ssp) green-

- 963 house gas concentrations and their extensions to 2500. *Geoscientific Model De-*
 964 *velopment*, 13(8), 3571–3605. Retrieved from [https://gmd.copernicus.org/](https://gmd.copernicus.org/articles/13/3571/2020/)
 965 [articles/13/3571/2020/](https://gmd.copernicus.org/articles/13/3571/2020/) doi: 10.5194/gmd-13-3571-2020
- 966 Meinshausen, M., Raper, S. C. B., & Wigley, T. M. L. (2011). Emulating coupled
 967 atmosphere-ocean and carbon cycle models with a simpler model, MAGICC6
 968 – part 1: Model description and calibration. *Atmospheric Chemistry and*
 969 *Physics*, 11(4), 1417–1456. doi: 10.5194/acp-11-1417-2011
- 970 Millar, R. J., Nicholls, Z. R., Friedlingstein, P., & Allen, M. R. (2017, jun). A
 971 modified impulse-response representation of the global near-surface air
 972 temperature and atmospheric concentration response to carbon dioxide
 973 emissions. *Atmospheric Chemistry and Physics*, 17(11), 7213–7228. doi:
 974 10.5194/acp-17-7213-2017
- 975 Millar, R. J., Otto, A., Forster, P. M., Lowe, J. A., Ingram, W. J., & Allen, M. R.
 976 (2015, Jul 01). Model structure in observational constraints on transient cli-
 977 mate response. *Climatic Change*, 131(2), 199-211. Retrieved from [https://](https://doi.org/10.1007/s10584-015-1384-4)
 978 doi.org/10.1007/s10584-015-1384-4 doi: 10.1007/s10584-015-1384-4
- 979 Morice, C. P., Kennedy, J. J., Rayner, N. A., & Jones, P. D. (2012, apr). Quantify-
 980 ing uncertainties in global and regional temperature change using an ensemble
 981 of observational estimates: The HadCRUT4 data set. *Journal of Geophysical*
 982 *Research: Atmospheres*, 117(D8), n/a–n/a. doi: 10.1029/2011jd017187
- 983 Morice, C. P., Kennedy, J. J., Rayner, N. A., Winn, J. P., Hogan, E., Killick, R. E.,
 984 ... Simpson, I. R. (2021). An updated assessment of near-surface tem-
 985 perature change from 1850: The hadcrut5 data set. *Journal of Geophysical*
 986 *Research: Atmospheres*, 126(3), e2019JD032361. Retrieved from [https://](https://agupubs.onlinelibrary.wiley.com/doi/abs/10.1029/2019JD032361)
 987 agupubs.onlinelibrary.wiley.com/doi/abs/10.1029/2019JD032361
 988 (e2019JD032361 2019JD032361) doi: <https://doi.org/10.1029/2019JD032361>
- 989 Murphy, J. M., Booth, B. B. B., Boulton, C. A., Clark, R. T., Harris, G. R., Lowe,
 990 J. A., & Sexton, D. M. H. (2014). Transient climate changes in a perturbed
 991 parameter ensemble of emissions-driven earth system model simulations.
 992 *Climate Dynamics*, 43(9), 2855–2885. Retrieved from [https://doi.org/](https://doi.org/10.1007/s00382-014-2097-5)
 993 [10.1007/s00382-014-2097-5](https://doi.org/10.1007/s00382-014-2097-5) doi: 10.1007/s00382-014-2097-5
- 994 Nicholls, Z., & Lewis, J. (2021, March). *Reduced Complexity Model Intercompari-*
 995 *son Project (RCMIP) protocol*. Zenodo. Retrieved from [https://doi.org/10](https://doi.org/10.5281/zenodo.4589756)
 996 [.5281/zenodo.4589756](https://doi.org/10.5281/zenodo.4589756) doi: 10.5281/zenodo.4589756
- 997 Nicholls, Z. R. J., Meinshausen, M., Lewis, J., Gieseke, R., Dommenges, D.,
 998 Dorheim, K., ... Xie, Z. (2020). Reduced complexity model intercompar-
 999 ison project phase 1: introduction and evaluation of global-mean tempera-
 1000 ture response. *Geoscientific Model Development*, 13(11), 5175–5190. Re-
 1001 trieved from <https://gmd.copernicus.org/articles/13/5175/2020/> doi:
 1002 10.5194/gmd-13-5175-2020
- 1003 O'Neill, B. C., Tebaldi, C., van Vuuren, D. P., Eyring, V., Friedlingstein, P., Hurtt,
 1004 G., ... Sanderson, B. M. (2016). The scenario model intercomparison project
 1005 (scenariomip) for cmip6. *Geoscientific Model Development*, 9(9), 3461–3482.
 1006 Retrieved from <https://gmd.copernicus.org/articles/9/3461/2016/> doi:
 1007 10.5194/gmd-9-3461-2016
- 1008 Rogelj, J., Meinshausen, M., & Knutti, R. (2012, Apr 01). Global warming under
 1009 old and new scenarios using ipcc climate sensitivity range estimates. *Nature*
 1010 *Climate Change*, 2(4), 248-253. Retrieved from [https://doi.org/10.1038/](https://doi.org/10.1038/nclimate1385)
 1011 [nclimate1385](https://doi.org/10.1038/nclimate1385) doi: 10.1038/nclimate1385
- 1012 Rogelj, J., Shindell, D., Jiang, K., Fifita, S., Forster, P., Ginzburg, V., ... et al.
 1013 (2018). Mitigation pathways compatible with 1.5°C in the context of sus-
 1014 tainable development. In G. Flato, J. Fuglestedt, R. Mrabet, & R. Scha-
 1015 effer (Eds.), *Global warming of 1.5 °C: an ipcc special report on the impacts*
 1016 *of global warming of 1.5 °C above pre-industrial levels and related global*
 1017 *greenhouse gas emission pathways, in the context of strengthening the global*

- 1018 *response to the threat of climate change, sustainable development, and ef-*
 1019 *forts to eradicate poverty* (p. 93–174). IPCC/WMO. Retrieved from
 1020 <http://www.ipcc.ch/report/sr15/>
- 1021 Sanderson, B. M., Wehner, M., & Knutti, R. (2017). Skill and independence weight-
 1022 ing for multi-model assessments. *Geoscientific Model Development*, 10(6),
 1023 2379–2395. Retrieved from [https://gmd.copernicus.org/articles/10/](https://gmd.copernicus.org/articles/10/2379/2017/)
 1024 [2379/2017/](https://gmd.copernicus.org/articles/10/2379/2017/) doi: 10.5194/gmd-10-2379-2017
- 1025 Schlesinger, M. E., Jiang, X., & Charlson, R. J. (1992). Implication of anthro-
 1026 pogenic atmospheric sulphate for the sensitivity of the climate system. In
 1027 *Climate change and energy policy: Proceedings of the international conference*
 1028 *on global climate change: Its mitigation through improved production and use*
 1029 *of energy [rosen, l. and r. glasser (eds.)]. amer. inst. phys., new york, ny, usa*
 1030 (pp. 75–108).
- 1031 Schwarber, A. K., Smith, S. J., Hartin, C. A., Vega-Westhoff, B. A., & Sriver, R.
 1032 (2019, nov). Evaluating climate emulation: fundamental impulse testing
 1033 of simple climate models. *Earth System Dynamics*, 10(4), 729–739. doi:
 1034 10.5194/esd-10-729-2019
- 1035 Sherwood, S. C., Webb, M. J., Annan, J. D., Armour, K. C., Forster, P. M., Har-
 1036 greaves, J. C., ... Zelinka, M. D. (2020). An assessment of earth's climate
 1037 sensitivity using multiple lines of evidence. *Reviews of Geophysics*, 58(4),
 1038 e2019RG000678. Retrieved from [https://agupubs.onlinelibrary.wiley](https://agupubs.onlinelibrary.wiley.com/doi/abs/10.1029/2019RG000678)
 1039 [.com/doi/abs/10.1029/2019RG000678](https://agupubs.onlinelibrary.wiley.com/doi/abs/10.1029/2019RG000678) (e2019RG000678 2019RG000678) doi:
 1040 10.1029/2019RG000678
- 1041 Simmons, A. J., Berrisford, P., Dee, D. P., Hersbach, H., Hirahara, S., & Thépaut,
 1042 J.-N. (2017). A reassessment of temperature variations and trends from
 1043 global reanalyses and monthly surface climatological datasets. *Quarterly Jour-*
 1044 *nal of the Royal Meteorological Society*, 143(702), 101–119. Retrieved from
 1045 <https://rmets.onlinelibrary.wiley.com/doi/abs/10.1002/qj.2949> doi:
 1046 10.1002/qj.2949
- 1047 Skeie, R. B., Berntsen, T., Aldrin, M., Holden, M., & Myhre, G. (2018, jun).
 1048 Climate sensitivity estimates – sensitivity to radiative forcing time series
 1049 and observational data. *Earth System Dynamics*, 9(2), 879–894. doi:
 1050 10.5194/esd-9-879-2018
- 1051 Skeie, R. B., Fuglestedt, J., Berntsen, T., Peters, G. P., Andrew, R., Allen, M., &
 1052 Kallbekken, S. (2017, feb). Perspective has a strong effect on the calculation
 1053 of historical contributions to global warming. *Environmental Research Letters*,
 1054 12(2), 024022. doi: 10.1088/1748-9326/aa5b0a
- 1055 Skeie, R. B., Peters, G. P., Fuglestedt, J., & Andrew, R. (2021). A future perspec-
 1056 tive of historical contributions to climate change. *Climatic Change*, 164(1),
 1057 24. Retrieved from <https://doi.org/10.1007/s10584-021-02982-9> doi:
 1058 10.1007/s10584-021-02982-9
- 1059 Smith, C. J., Forster, P. M., Allen, M., Leach, N., Millar, R. J., Passerello, G. A.,
 1060 & Regayre, L. A. (2018, jun). FAIR v1.3: a simple emissions-based impulse
 1061 response and carbon cycle model. *Geoscientific Model Development*, 11(6),
 1062 2273–2297. doi: 10.5194/gmd-11-2273-2018
- 1063 Smith, C. J., Kramer, R. J., Myhre, G., Alterskjær, K., Collins, W., Sima, A.,
 1064 ... Forster, P. M. (2020). Effective radiative forcing and adjustments in
 1065 cmip6 models. *Atmospheric Chemistry and Physics*, 20(16), 9591–9618. Re-
 1066 trieved from <https://acp.copernicus.org/articles/20/9591/2020/> doi:
 1067 10.5194/acp-20-9591-2020
- 1068 Smith, C. J., Kramer, R. J., Myhre, G., Forster, P. M., Soden, B. J., Andrews,
 1069 T., ... Watson-Parris, D. (2018). Understanding rapid adjustments to di-
 1070 verse forcing agents. *Geophysical Research Letters*, 45(21), 12,023–12,031.
 1071 Retrieved from [https://agupubs.onlinelibrary.wiley.com/doi/abs/](https://agupubs.onlinelibrary.wiley.com/doi/abs/10.1029/2018GL079826)
 1072 [10.1029/2018GL079826](https://agupubs.onlinelibrary.wiley.com/doi/abs/10.1029/2018GL079826) doi: 10.1029/2018GL079826

- 1073 Su, X., Shiogama, H., Tanaka, K., Fujimori, S., Hasegawa, T., Hijioka, Y., ... Liu,
1074 J. (2018). How do climate-related uncertainties influence 2 and 1.5° c path-
1075 ways? *Sustainability science*, *13*(2), 291–299.
- 1076 Su, X., Tachiiri, K., Tanaka, K., Watanabe, M., & Kawamiya, M. (2020). Source
1077 attributions of radiative forcing by regions, sectors, and climate forcers. *arXiv*
1078 *preprint arXiv:2009.07472*.
- 1079 Su, X., Takahashi, K., Fujimori, S., Hasegawa, T., Tanaka, K., Kato, E., ... Emori,
1080 S. (2017). Emission pathways to achieve 2.0 c and 1.5 c climate targets.
1081 *Earth's Future*, *5*(6), 592–604.
- 1082 Tokarska, K. B., Stolpe, M. B., Sippel, S., Fischer, E. M., Smith, C. J., Lehner,
1083 F., & Knutti, R. (2020). Past warming trend constrains future warming in
1084 cmip6 models. *Science Advances*, *6*(12). Retrieved from [https://advances](https://advances.sciencemag.org/content/6/12/eaaz9549)
1085 [.sciencemag.org/content/6/12/eaaz9549](https://advances.sciencemag.org/content/6/12/eaaz9549) doi: 10.1126/sciadv.aaz9549
- 1086 Tsutsui, J. (2017, jan). Quantification of temperature response to CO2 forcing in at-
1087 mosphere–ocean general circulation models. *Climatic Change*, *140*(2), 287–305.
1088 doi: 10.1007/s10584-016-1832-9
- 1089 Tsutsui, J. (2020, apr). Diagnosing transient response to CO2 forcing in coupled
1090 atmosphere–ocean model experiments using a climate model emulator. *Geo-*
1091 *physical Research Letters*, *47*(7). doi: 10.1029/2019gl085844
- 1092 Uhe, P., Otto, F. E., Rashid, M. M., & Wallom, D. C. (2016). Utilising amazon web
1093 services to provide an on demand urgent computing facility for climatepredic-
1094 tion. net. In *2016 ieee 12th international conference on e-science (e-science)*
1095 (pp. 407–413).
- 1096 van Vuuren, D. P., Lowe, J., Stehfest, E., Gohar, L., Hof, A. F., Hope, C., ...
1097 Plattner, G.-K. (2011, jan). How well do integrated assessment mod-
1098 els simulate climate change? *Climatic Change*, *104*(2), 255–285. doi:
1099 10.1007/s10584-009-9764-2
- 1100 Vega-Westhoff, B., Sriver, R. L., Hartin, C. A., Wong, T. E., & Keller, K. (2019,
1101 jun). Impacts of observational constraints related to sea level on estimates of
1102 climate sensitivity. *Earth's Future*, *7*(6), 677–690. doi: 10.1029/2018ef001082
- 1103 von Schuckmann, K., Cheng, L., Palmer, M. D., Hansen, J., Tassone, C., Aich,
1104 V., ... Wijffels, S. E. (2020). Heat stored in the earth system: where
1105 does the energy go? *Earth System Science Data*, *12*(3), 2013–2041. Re-
1106 trieved from <https://essd.copernicus.org/articles/12/2013/2020/> doi:
1107 10.5194/essd-12-2013-2020
- 1108 Weaver, C. P., Lempert, R. J., Brown, C., Hall, J. A., Revell, D., & Sarewitz, D.
1109 (2013). Improving the contribution of climate model information to decision
1110 making: the value and demands of robust decision frameworks. *WIREs Cli-*
1111 *mate Change*, *4*(1), 39-60. Retrieved from [https://onlinelibrary.wiley](https://onlinelibrary.wiley.com/doi/abs/10.1002/wcc.202)
1112 [.com/doi/abs/10.1002/wcc.202](https://onlinelibrary.wiley.com/doi/abs/10.1002/wcc.202) doi: 10.1002/wcc.202